2019-01-01

Development and Characterization of Polyethylene Terephthalate (PET)-Cotton Natural Fiber-Reinforced Composites From Waste Materials

Israel Alejandro Carrete
University of Texas at El Paso, iacarrete@gmail.com

DEVELOPMENT AND CHARACTERIZATION OF POLYETHYLENE TEREPHTHALATE (PET)-COTTON NATURAL FIBER-REINFORCED COMPOSITES FROM WASTE MATERIALS

ISRAEL ALEJANDRO CARRETE

Master's Program in Metallurgical and Materials Engineering

APPROVED:

David A. Roberson, Ph.D., Chair

Binata Joddar, Ph.D.

Adeeba A. Raheem, Ph.D.

Stephen Crites, Ph.D.
Dean of the Graduate School

Dedication

Para mi familia, que siempre me ha apoyado en todos mis esfuerzos y para Gaia, con esperanzas de comenzar el proceso de sanación.

DEVELOPMENT AND CHARACTERIZATION OF POLYETHYLENE TEREPHTHALATE (PET)-COTTON NATURAL FIBER-REINFORCED COMPOSITES FROM WASTE MATERIALS

by

ISRAEL ALEJANDRO CARRETE, B.Sc.

THESIS

Presented to the Faculty of the Graduate School of

The University of Texas at El Paso

in Partial Fulfillment

of the Requirements

for the Degree of

MASTER OF SCIENCE

Department of Metallurgical, Materials, and Biomedical Engineering

THE UNIVERSITY OF TEXAS AT EL PASO

May 2019

Acknowledgements

No journeys are completed alone, and I would like to thank everyone that was a part of this journey with me. First, I would like to thank Dr. Roberson for his mentorship throughout my time at the University of Texas at El Paso and being an example that helping others out of the goodness of one's heart has its rewards. Without Dr. Roberson's support at UTEP, I would not have been able to take on an endeavor that as close to my heart as this study is, so I thank him for pushing me, teaching me, and allowing me to be a part of the extended family that is the Polymers Extrusion Lab.

Extended thanks go out to my family for always supporting my endeavors and encouraging me to leave my comfort zone to grow. Para mis padres y mi Tata, que siempre nos han dado más de lo que podríamos pedir con un ejemplo de humildad y servicio al prójimo y para mis hermanxs (incluyendo a Mayela) con cuyo apoyo moral siempre puedo contar para seguir adelante. Y para los Tarin que siempre me animan a ver el mundo más allá de lo mío sin dejarme olvidar mis raíces.

To my colleagues at UTEP, a support group that made the load of completing this endeavor nearly enjoyable, I thank you immensely because this would not be complete without any of you. To the past and present of the extended Polymer Extrusion Lab family: Kevin, Evelyn, Diego, Truman, Paulina, Fabian, Sabastian, Lety, Heidi, Gil, and Paco. Thank you for your friendship and your time. Finally, to everyone that lent me a helping hand out of the kindness of their hearts, Iris, Francelia, Kim, Ale, and Jackie. Your contributions helped put all of this together and for that I am ever grateful.

Abstract

Unprecedented levels of production and consumption have caused a rapid exhaustion of the Earth's virgin resources, which is coupled with a fast accumulation of contaminants in the form of solid waste, especially in landfills. Two significant landfill constituents come from textile waste and discarded plastic bottles. Since there is a finite amount of space that can be feasibly used for landfills, solutions that make use of these post-consumer products are imperative. This study presents one possible solution by using surface modifications of cotton fibers to produce a natural fiber-reinforced polymer composite (NFRPC) from post-consumer textile waste and polyethylene terephthalate (PET) water bottles as pseudo raw materials. This novel composite material in the form of a monofilament feedstock for 3D printing toughened the recycled PET (RPET) matrix. The study follows the processing of the NFRPC by hydrolyzing functionalizing fibers from white denim cloth (as a representation of bleached fibers) as well as fibers from post-consumer denim jeans that contain indigo-dye. Characterization techniques such as dynamic mechanical analysis, attenuated total reflectance, impact tests, melt flow index, and scanning electron microscopy were all preformed on the various NFRPC states to verify the efficiency of the functionalization process and interfacial adhesion.

Table of Contents

Acknowledgements v

Abstract vi

Table of Contents vii

List of Tables ix

List of Figures x

Chapter 1: Motivation 1

1.1 Plastic Waste 3

1.2 Textile Waste 5

Chapter 2: Background Information 8

2.1 Polymer Background 8

2.1.1 Rheology and Processing Parameters 9

2.1.2 Additives 10

2.2 Poly(ethylene Terephthalate) – PET 11

2.3 Cotton 13

2.4 Indigo Dye 15

Chapter 3: Composite Materials 17

3.1 Polymer Matrix Composites 19

3.2 Natural Fiber-Reinforced Polymers (NFRPs) 19

3.2.1 Fiber Properties 20

Chapter 4: Additive Manufacturing 23

4.1 Fused Deposition Modeling (FDM) 23

4.1.1 Extrusion 24

4.2 Printing Direction – mechanical Properties and Limitations 26

4.3 Potential for Composites 27

Chapter 5: Materials & Methods 28

5.1 Materials 28

5.2 Procedures 28

5.2.1 Melt Flow Index (MFI) 30

5.2.2 RPET Extrusions....31
5.2.2.1 Cotton Fiber Retrieval....32
5.2.2.2 Cotton Functionalization....34
5.2.2.3 Composite Extrusion....35
5.2.3 Printing Test Specimens....37
5.2.4 Attenuated Total Reflectance (ATR)....39
5.2.5 Dynamic Mechanical Analysis (DMA)....39
5.2.6 Impact Test....40
5.2.7 Fractography (SEM)....40
Chapter 6: Results & Discussion....42
6.1 Melt Flow Index....42
6.2 Attenuated Total Reflectance (ATR)....42
6.3 Dynamic Mechanical Analysis....44
6.4 Izod Impact Tests....45
6.5 Scanning Electron Microscopy (SEM)....48
Chapter 7: Conclusions....54
7.1 Future Works....56
7.1.1 Applications for Cotton-PET NFRPC....57
References....59
Curriculum Vita....65

List of Tables

Table 1: Average measured MFI (HP vs. NHP) 31
Table 3:Extrusion parameters for indigo cotton in the Collin extruder 38
Table 4: MFI results for all three filaments 42
Table 5: Summary of DMA findings for RPET and RPET-WC 45
Table 6: Average impact test results for RPET and PRET-WC 46

List of Figures

Figure 1: Solid waste figures in the U.S. (2015) [6] 2
Figure 2: Example of molecular arrangement in crystalline polymers [25] 9
Figure 3: Schematic of PET polycondensation process [33] 12
Figure 4: Thermal degradation of ester bonds [33] 13
Figure 5: Cellulose chemical structure [36] 14
Figure 6: Isolation of cellulose fiber through hydrolysis [37] 15
Figure 7: Indigo chemical structure [40] 15
Figure 8: Composite reinforcement configurations [43] 18
Figure 9: Hot-melt extrusion system [64] 25
Figure 10: a) Twin-screw assembly [64] b) configurations and c) pressure distribution [86] 26
Figure 11: a) First attempt at extruding recycled PET (RPET) with air cooling b) Comparison of 1) HP and 2) NHP RPET 30
Figure 12: HP vs. NHP MFI results 31
Table 2: RPET extrusion parameters 32
Figure 13: RPET 1.75mm filament 32
Figure 15: RPET-10 vol% white cotton mixture 35
Figure 16: Filabot EX2 extrusion setup 36
Figure 17: 1.75mm composite filaments - a) RPET-10 vol% WC and b) RPET-10 vol% IC 36
Figure 18: Representative DMA specimens for a) RPET b) RPET-WC and c) RPET-IC 39
Figure 19: ATR spectra for all composite filaments and their constituents 43
Figure 20: Shortened section of the ATR spectra to point out the presence of a new peak (red bar) in the composite materials. 44
Figure 21: Representative DMA curves for a) RPET and b) RPET-WC 45
Figure 22: Representative RPET fracture surface near the v-notch at a) low magnification and b) high magnification 47
Figure 23: Representative RPET-WC fracture surface near the v-notch at a) low magnification and b) high magnification 47
Figure 24: RPET-WC hinge fracture 47
Figure 25: RPET filament fracture surfaces 48
Figure 26: Low magnification RPET-WC a) top and b) bottom fracture surfaces 49
Figure 27: High magnification RPET-WC a) top and b) bottom fracture surfaces 49
Figure 28: High magnification RPET-WC fiber seen in Figure 27b at two magnifications 50
Figure 29: Low magnification RPET-IC fracture surfaces – a) and b) foam filament c) dark filament d) agglomerated filament and e) high magnification image of d) 52

Chapter 1: Motivation

Consumerism is a quotidian part of life, especially in the United States. While this was not always the case, the current consumption trends date back to the post war era in which unprecedented levels of production had to be balanced by constant consumption. In Jim Hightower's *War on Waste*, the author provides an insight that reveals a change in attitude that took place after World War II. The war marked a turning point from principles of conservation to support troops abroad to a rampant consumption used to keep up with production levels. Increased consumption levels were implemented to continue economic growth avoid a second Great Depression [1].

Manufacturers began producing at rates that consumers were unable to keep up with, so advertisers stepped in to "psychologically condition []" consumers into buying more [2]. At the time of his critique of consumerism in 1960, Vance Packard was convinced that the accelerated rate of consumption was going to have negative consequences on the United States. Throughout his book, *Waste Makers*, Packard details how advertisers changed consumer perceptions toward consumption and even helped normalize spending patterns that are still visible to this day. The most relevant piece of his input to this work is Packard's commentary on planned obsolescence – the intentional premature failure of a product to promote repeated purchases [3]. Over half a century after this criticism, however, planned obsolescence has only become more common, with companies limiting repairs and making an upgrade or replacement more accessible than fixing a product. Aladeojebi [4] argues that there is even a perceived loss of value when companies release successive upgrades to a product, even if the benefit of upgrading is marginal, which in turn promotes repeat purchases. In fact, constant upgrades ties into the idea of status goods,

whereby the purchase of an expensive or new product reflects a higher socioeconomic standing, which is another driving force for frequent purchases [5].

Whatever the cause of the apparent devaluing of a product may be, its disposal inevitably followed. Over time, an increasing number of products were discarded, but little action was taken to properly dispose of or recycle these durable goods. Thus, unprecedented levels of solid waste accumulated and are still seen in landfills. According to the Environmental Protection Agency (**Figure 1**), in the United States alone, 137.7 million tons of solid waste were discarded in 2015, much of which has been encouraged by single use consumption and planned obsolescence [6]. Half a century later, wasteful practices and uninhibited consumption are being called into question since the consequences of improper disposal techniques are evident in the environment and ecology. There is no cure-all or immediate solution for such an issue, but steps must be taken to attempt to restore the planet's health. The following study offers one such step by presenting a path to reusing textile and plastic waste from post-consumer clothes and PET water bottles found in landfills, respectively, as *pseudo raw materials* for a natural fiber-reinforced polymer matrix composite 3D printing filament.

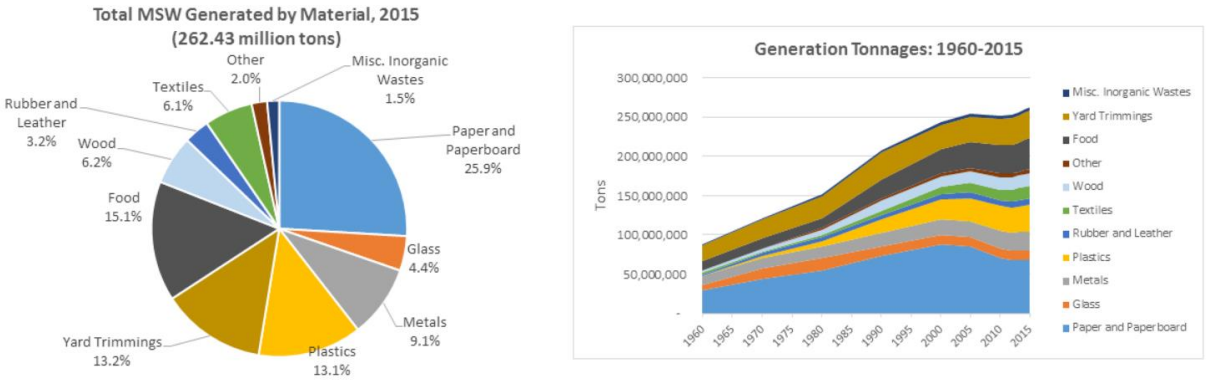

Figure 1: Solid waste figures in the U.S. (2015) [6]

1.1 PLASTIC WASTE

Before going into the production of the composite, it might help to understand the magnitude of the issue at hand by first looking at the statistics for the two materials being used here – cotton from post-consumer textile waste and polyethylene terephthalate (PET) plastic from water bottles – and their effects on the environment. As far as plastics go, the Environmental Protection Agency reported in 2015 that nearly 19% of landfill waste (26 million tons) were discarded in the United States during that year alone [6]. **Figure 1** shows the amount of waste that ends up in landfills but does not take into consideration the waste produced that has a different destination than landfills (i.e. the amount that ends up in the oceans or is recycled). Another 2015 EPA report focused on data pertaining to plastics and notes that a total of 14 million tons of plastic were discarded in the packaging industry alone, 9% of which were recovered. However, it is noted that PET water bottles and jars had a recycling rate of nearly 30% that year. [7]

The remaining disposed plastics have different end points. One area of concern is the accumulation of plastic in oceans, as they more directly affect wildlife. A study by Jambeck et al. published in 2010 dives into this issue and attempts to calculate the amount of plastic waste accumulated in oceans in coastal regions around the world [8]. An analysis of plastic production and waste management in populations 50 km from the coast concluded that, of the 275 million metric tons of waste produced in these populations, between 4.8 and 12.7 million metric tons entered the ocean. [8] Since the plastic entering the ocean is buoyant (due to the specific gravity of most polymers being close to 1), it remains near the surface, where the currents break it up into microplastic debris that is ingested by wildlife, leading, in many cases to the death of the marine life, birds, or even mammals [9]. Fries et al. further this investigation and identify the types of microplastics found in marine environments, as well as their impact on marine life. For

example, additive plasticizers found in ocean plastics often include phthalates, which disrupt endocrine (hormonal) systems in invertebrates and fish, affecting the reproductive systems and development of these animals [10].

Cauwenberghe and Janssen showed that microplastics are present in two types of shellfish used for human consumption and even estimated the amount of plastic ingested by regular seafood eaters to be around 11,000 microplastic particles per year [11]. Indirect digestion of plasticizers that disrupt invertebrate hormonal systems also affect those of humans. Because of their size, fish easily ingest microplastics, but because synthetic fibers have existed for less than a century, bacteria do not easily decompose them and humans that eat these fish also ingest the microplastics [12]. Plastics such as PET are not necessarily harmful on their own, but the chemicals used to plasticize them have been "correlated with infertility, recurrent miscarriages, feminization of male fetuses, early-onset puberty, early-onset menopause, obesity, diabetes, reduced brain development, cancer, and neurological disorders such as early-onset senility in adults and reduced brain development in children" [12].

Evidently, the issue at hand is global and multifaceted. No one solution will address everything, but this study aims to take a step towards reversing the accumulation of solid waste by offering a way to recycle PET bottles at a better rate than what was mentioned above. Although PET bottles are within the class of plastics considered to be recyclable, they are, for the most part, not recycled. With one million plastic bottles consumed per minute globally (as of 2017), 91% are not recycled [13]. At this rate, plastic waste will evolve from being an environmental issue into a medical one unless something is done to address it.

1.2 TEXTILE WASTE

While masses such as the Great Pacific garbage patch are well known, the analogous effects of textile waste are largely underestimated. Textile waste refers to "all types of garments or household articles made of textiles that the owner no longer needs and decides to discard" [14]. Municipal solid waste (MSW) figures seen in **Figure 1** show that textile waste amounted to 7.6% of landfill waste (about 10.5 million tons) in 2015 alone [6]. Such an expansive accumulation was enhanced by industrialization (which made it easier to mass produce textiles) and obsolescence promoted by passing fashion trends [15]. Despite the vast number of discarded textiles in the US on an annual basis, only 15% is diverted from landfills even though virtually all textile waste can be reused in some way – even as incineration for fuel. The improper disposal of waste is owed in part to the association of clothes as an extension of the owner's self [16]. The language involving clothes and waste is partially to blame for these attitudes. Since new is often associated with cleanliness, used clothes are perceived to be dirty and therefore unworthy of another life once the original owner no longer has a use for it and recycling is not considered an option in many cases [17].

Cleanliness impacts the lifecycle of textiles greatly since the value of a garment plummets when stains are present. In fact, unremovable stains almost inevitably result in a garment that could have been recycled otherwise ending in a landfill, where its value is entirely lost [18]. The 34% of garments that are not discarded and manage to get recycled become a part of the secondhand clothing industry [18]. Returning to the extended sense of self that is perceived to inhabit an article of clothing, some people prefer to donate a garment, not because of its environmental impact, but because that part of themselves continues to live on in someone else. A large portion of donated clothes end up being resold if their quality is not affected very

much. However, due to the massive intake of clothes, not all of them can be resold on a local level and are thus shipped overseas, where they are sold in developing nations in bales of varying values [19].

The notion of treating clothes as a part of the owner rather than a consumer product certainly affects how it will be treated at the end of a garment's lifecycle, for it cannot be divorced from its owner and seen for what it is: a collection of fibers and fabrics that have been treated and assembled into a particular aesthetic and function [20]. In fact, the treatment and processing of these fibers before consumer use is one of the largest reasons why reusing them is urgent. For example, the multitude of colors present in garments are all obtained through a dyeing process, which is one of the largest water contaminants due to alkalines and toxic chemicals used to do so dye fabrics. The process begins with desizing - a removal of starch from fibers such as cotton through hydrolysis or oxidation with chemicals. Subsequently, the fibers are bleached and neutralized with water before dyeing. By adding the dye, the water is no longer reusable unless it is treated, but it usually goes off into larger bodies of water where it continues to contaminate and harm wildlife. Finally, a variety of finishes are applied to change the properties or aesthetics of the fibers with the help of additives [21]. All in all, the process of dyeing fibers is one of the largest contaminants in textile production, which could be addressed with either water treatment, or reducing the treatment of virgin resources by reusing those that have already been processed.

Despite the impact of dyeing on the environment, contamination from textile wastes can be seen both when the garments are still in use as well as when they enter the post-consumer stage. The washing of clothes often leads to wearing that releases microplastic fibers, which end up in waterways as well. This is especially true of synthetic fibers such as polyesters, acrylic

fabrics, and blends. [22] The additives used to make textile garments last longer are often released as microplastics that negatively affect marine life by disrupting endocrine systems of organisms [10]. These same coatings that alter the properties of the garment also decrease the rate of deterioration, which makes the garment more durable while also making it last a much longer time before biodegrading. Given that textile garments are discarded within relatively quick cycles, the finishes used to make them more durable further promotes accumulation of waste in landfills [23].

In response to the gargantuan task of reducing the volume of waste in landfills and even using the materials found there as a pseudo-raw material with which to create something new, this study aims to incorporate elements of both cotton fibers from post-consumer denim jeans and PET from plastic bottles into a composite filament to be used for 3D printing. The following chapter will focus on background information regarding the properties of thermoplastics (specifically PET), cotton, and composite materials that will serve as a guide to the development of the composite filament.

Chapter 2: Background Information

2.1 Polymer Background

The term polymer refers to a subclass of engineering materials that is composed of organic macromolecules whose carbon backbone contains repeating units of branches and molecules known as *mers*. Depending on the configuration of such branches, the classification of the polymer changes, along with its properties. Of the three main subcategories – thermoplastics, thermosets, and elastomers – the kind that is most known is the first, often simply called "plastics". Thermosetting polymers refer to those that branch in such a way that the molecular arrangement forms a series of networks. The network configuration restricts molecular chain movement and results in a very rigid material that is often cured at high temperatures but cannot be reversed or reprocessed. Elastomers, on the other hand, are extremely flexible and elastic, which means they can be highly deformed and still return to the original shape [24].

The final subcategory of polymers, thermoplastics, refers to polymers that become soft and viscous at high temperatures, meaning that that they can be processed and reprocessed. These thermoplastics ("plastics" from here on) are the focus of this study because they are the most readily recyclable under appropriate temperature conditions. Water bottles (made of PET) fall under this category. Plastics' "recyclability" is due to the linear or simply branched backbone structures that are held together by weak van der Waals forces, which break down with heat to form a viscous fluid.

The linear structure of thermoplastics allows for limited crystallinity to occur when the chains of macromolecules fold into parallel plate as shown in **Figure 2** [25]. However, the degree of crystallinity is defined by side chains. If these chains do not fit into the ordered structure of the lamellae, an amorphous section forms adjacent to the crystalline one. More

complex polymers with large pendant groups or large degrees of branching cannot exhibit any crystalline behavior and are purely amorphous. The degree of crystallinity differs depending on the type of polymer and their molecular orientation, which affects several properties of the material. For example, high crystallinity leads to a stiffer material that exhibit a much higher melting (or transition) temperature, whereas a purely amorphous material is much softer, but with a higher impact resistance.

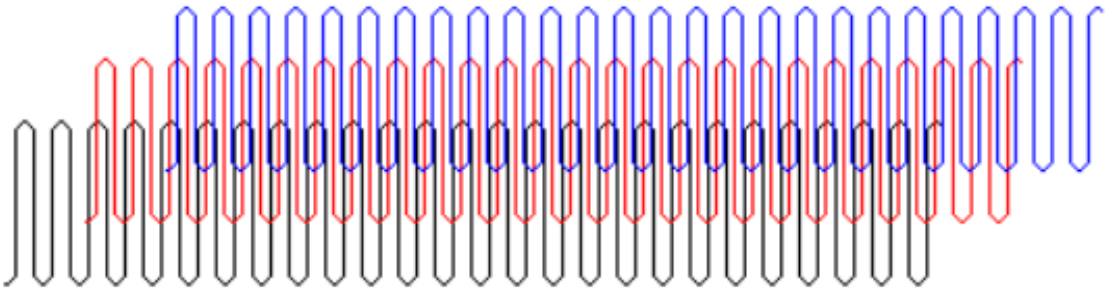

Figure 2: Example of molecular arrangement in crystalline polymers [25]

Despite the differences in rigidity between the crystalline and amorphous portions of a polymer, there exists a temperature range below which the amorphous sections transition from being viscous and rubbery in nature to a more rigid "glassy" state. This glass transition temperature, T_g, varies for every polymeric system, but it helps determine the properties that will be displayed under a certain service temperature. Equally important to additive manufacturing is the melting temperature T_m, which occurs when the molecules in the crystalline region become disordered once more and the solid becomes a less viscous fluid [26].

2.1.1 Rheology and Processing Parameters

Transitional properties of plastic systems are imperative to understanding processing parameters. Given that a plastic's processability depends on its intrinsic viscosity and whether it

is glassy or rubbery, the rheology of the system must be understood. Rheological studies, such as a melt flow index (MFI) relate to how a material will flow. In particular, a polymer's ability to flow depends on the crystallinity and the molecular mass of its chains. Though a direct relation has yet to be determined, it is understood that, the larger the chains are, the more the plastic resists flow and behaves like a viscous material [27]. Similarly, a high flow rate in the melt can be correlated to a small molecular mass [28]**.** Molecular mass and melt flow also affect mechanical properties, where the larger molecular masses lead to a higher impact strength while lowering the yield strength, stiffness, and softening points of the system [29].

Molecular chain size is also a limiting factor to the recyclability of a material. Whether polymers are processed through injection molding, compression molding, or extrusion, viscosity is essential to obtaining the desired shape. However, each thermal cycle used to reshape thermoplastics decreases the size of the chains and lowers viscosity because shear is introduced. The mixture of shear and high temperatures leads to the scission of some chains, which will inevitably decrease viscosity and make processing more difficult [29]. Attempts to facilitate the recycling of plastics have included adding monomers or chain extenders to counteract the chain scission [30].

2.1.2 Additives

Additives represent a set of chemical reagents that are added to a polymer to achieve a variety of properties. Additives include the following: 1) fillers and reinforcements (to be discussed further in Ch. 3); 2) plasticizers; 3) colorants; and 4) stabilizers. Inexpensive fillers can reduce cost of manufacturing by lowering the percentage of an expensive polymer matrix with inexpensive filler while reinforcements strengthen polymers or alter other mechanical properties.

Plasticizers lower glass transition temperatures and make materials less brittle. Colorants dye the plastics a certain color while stabilizers prevent degradation [31].

Since polymers are synthetic in nature, they do not undergo biodegradation as easily as an organic compound might. In other words, naturally occurring micro-organisms do not easily decompose synthetic polymers. This is especially true with additives used specifically to benefit the longevity of a polymer. For example, in the process of recycling plastics, chain extenders are often used to overcome the effects of chain scission resulting from multiple heat and shear cycles. However, increasing the life of a material that takes anywhere between decades to centuries to decompose also has adverse effects on the environment under which it decomposes, such as the landfills or oceans that these plastics end up in. Marine life is particularly sensitive to plasticizers given that organisms in this habitat end up ingesting plastic debris whose plasticizers disrupt their endocrine system [10]. Thus, although plasticizers are used to cater towards a specific effect in a plastic, they can also be detrimental to the environment.

2.2 POLY(ETHYLENE TEREPHTHALATE) – PET

Now that a general overview of polymers and plastics has been established, a deep dive into the focus of this study can be taken. This section will focus on poly(ethylene terephthalate), the most widely used polyester, also known as PET. Best known for its uses in the textile and bottle industry, PET is the plastic that is used for most plastic water bottles and food containers. As the name implies, polyesters contain an ester group as a major structural component, but they can also be identified through the reactions that bring them about – the polycondensation of a glycol group and a difunctional carboxylic acid [32]. At a time before World War II, when plastics were being more seriously investigated, J.R. Whinfield and Dickson independently created polyester fibers from terephthalic acid and ethylene glycol, for which they filed a patent

in 1941 [32]. However, a simultaneous discovery of PET in du Pont led to a widespread use of PET by the 1960s. Expanding the use of this material from a fiber former proved difficult at first, especially in injection molding, because of slow crystallization. However, by 1970, blow molding was implemented to make the first plastic bottles, and ever since, then, PET has been the plastic to use for such a job [32].

As a polyester, PET is formed through condensation – the combination of two molecules that results in the release of a small molecule such as water. In the case of PET, ethylene glycol and terephthalic acid come together in step growth. As seen in **Figure 3**, the first step is an esterification/hydrolysis process whereby the monomer of PET, bis-hydroxyethyl terephthalate (BHET), is produced as a prepolymer and water is released. Then, polycondensation occurs, and a transesterification reaction in the melt polymerizes the BHET monomers with ethylene glycol as a byproduct [33].

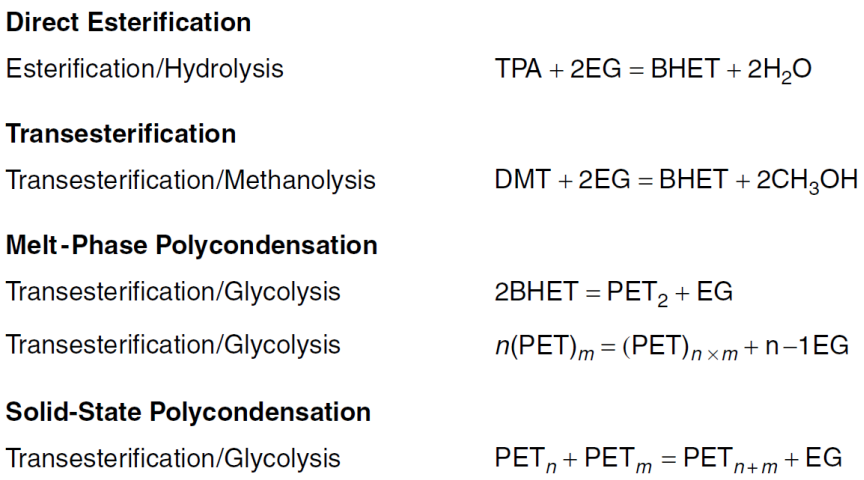

Figure 3: Schematic of PET polycondensation process [33]

The polymerized product then exists in two grades whose intrinsic viscosity and molecular weight differ. The first grade, used primarily for fiber applications (such as those used in textiles) also looks optically different, as TiO_2 is used to de-luster the polymer. The other

grade, used for bottle applications, has a different amount of co-monomers, stabilizers, and colorants. [34] Colorants can help prevent evidence of yellowing can result both from thermal degradation during processing, as well as oxidative degradation [33]. Oxidative degradation refers to the crosslinking or degradation of polymers when exposed to atmospheres containing oxygen [35]. On the other hand, thermal degradation is a major problem in PET that arises at temperatures above the melting point, which can occur even during synthesis or processing. Degradation begins with the scission of an ester bond, which can lead to the formation of acetaldehyde, which yellows the polymer and affects the taste of food in contact with the polymer [34]**.** Chain scission also reduces thermal stability and leads to a drop in intrinsic viscosity due to the shorter length of chains. A sample of the mechanism through which polyesters degrade thermally is shown in **Figure 4**.

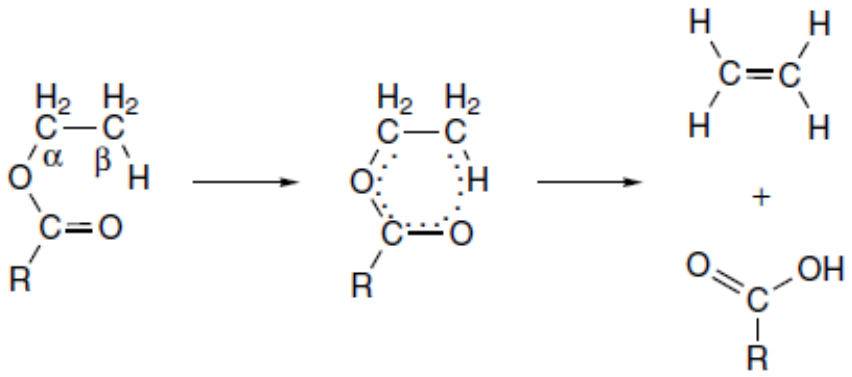

Figure 4: Thermal degradation of ester bonds [33]

2.3 COTTON

Cotton as it is used in textiles is largely derived from the plant *Gossypium hirsutum L.*, which produces naturally white cotton fibers [36]. Cotton fibers are composed of cellulose (**Figure 5**), the most widespread biopolymer in the world, which exists in plants, animals and even bacteria.

Cellulose is made up of an amorphous region and a needle-like microcrystalline region often referred to as a cellulose whisker [37].

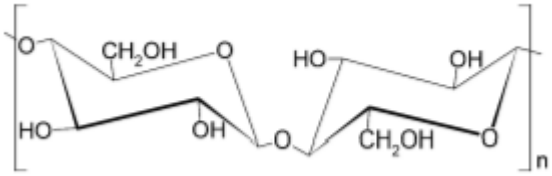

Figure 5: Cellulose chemical structure [36]

The main function of this biopolymer is to reinforce, a role which is seen clearly in the cell walls of plants. These reinforcing abilities make it an attractive alternative to inorganic fiber reinforcers in polymer matrix composites. Furthermore, organic and natural fiber reinforcers such as cellulose whiskers lower density and cost of polymers while increasing biodegradability and renewability. Thus, there have been various attempts at making polymer matrix composites after hydrolyzing cotton fibers in acid in order to dissolve the amorphous region of cellulose and leave behind only its micro crystallites. [37], [38], [39]

Figure 6 depicts the isolation of a cellulose microfibril through sulfuric acid hydrolysis. Acid hydrolysis removes the amorphous regions in cellulose, leaving only a crystalline whisker made up of a linear chain held together by strong bonds. [36], [40] The properties of the whisker depend highly on the source of cellulose, such as cotton, the time and temperature of exposure to sulfuric or hydrochloric acid for hydrolysis since this process relies on the diffusion of acid to cleave the glycosidic bonds in cellulose and remove the amorphous region [38]. Overexposure to the acid and processing temperatures above 230^{o}C may degrade and even decompose the fibers, so processing conditions must be optimized to properly benefit from cotton fibers as a reinforcement material.

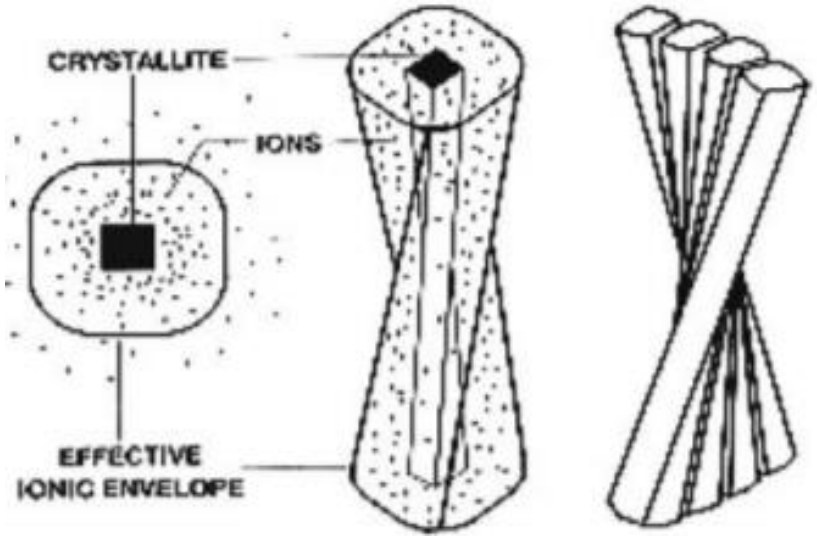

Figure 6: Isolation of cellulose fiber through hydrolysis [37]

2.4 INDIGO DYE

Indigo dye is the leading textile dye (primarily used for blue jeans) that is produced from *Indigofera tinctorial* for thousands of years throughout the world. Strong inter and intramolecular bonds give the dye a high melting point of 390^{o}C [41].Historically, indigo and similar natural dyes like Tyrian purple have been used for thousands of years. The extraction of the dye from the original plant source inspired the modern synthetic chemical industry given that the dye was produced by altering the chemical present in plants through oxidation [41]. The resulting indigo dye's structure is shown in **Figure 7**.

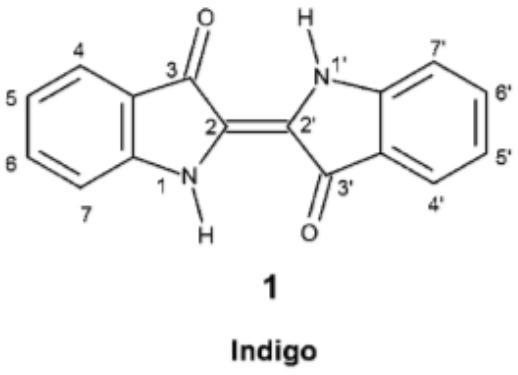

Figure 7: Indigo chemical structure [40]

Hydrogen bonding in the molecule is responsible for many characteristics ranging from the intense color to its low solubility in organic solvents. In the solid state, indigo molecules hydrogen-bond to four neighbors, two of which are π-stacked and further reinforced by more hydrogen bonds [41].The reinforced bonds and high melting point of the dye make indigo-dyed cotton fibers an even more attractive reinforcement if proper processing conditions can be attained, but for that to occur, it is important to understand what makes a composite material successful.

Chapter 3: Composite Materials

Composite materials are effectively the mixture of distinct engineering materials whose combination yields a combination of properties from each of the constituents. In most cases, there are two phases in the composite, a matrix and a reinforcer, that interact to improve mechanical and physical properties or even the cost of the material. In some cases, a ductile or soft matrix acts as a binder or glue to the high strength reinforcing particles that increase strength while reducing density. In these cases, the matrix transfers stress to the reinforcing particles while protecting them from environmental conditions such as oxidation. Hard materials are often toughened when ductile materials are imbedded to resist brittle crack propagation [42].

There are various types of reinforcement configurations depending on matrix-reinforcer interactions, such as fiber reinforcements (continuous and discontinuous) particle reinforcement and layered materials (shown in **Figure 8**). Fiber reinforcement entails high strength fibers that are imbedded in a softer matrix to improve its mechanical properties. Fibers within the matrix may have different configurations. The first is that of continuous fibers that are aligned parallel to each other, which introduces anisotropy as the effects of reinforcement are greatest along the length of the fiber. On the other hand, discontinuous fibers are smaller fibers that may either be aligned, yielding a similar anisotropic effect as continuous fibers, or they may have a random orientation, which yields a more uniform reinforcement throughout the matrix, albeit a smaller one compared to the aligned fibers.

Layered or laminated composites have the reinforcing phase layered in different orientations to homogenize properties. Lastly, particle reinforcement is a result of a reinforcement phase that is not necessarily shaped like a fiber and whose distribution is thus more random [43]. As can be expected, the reinforcing phase plays a critical role in the

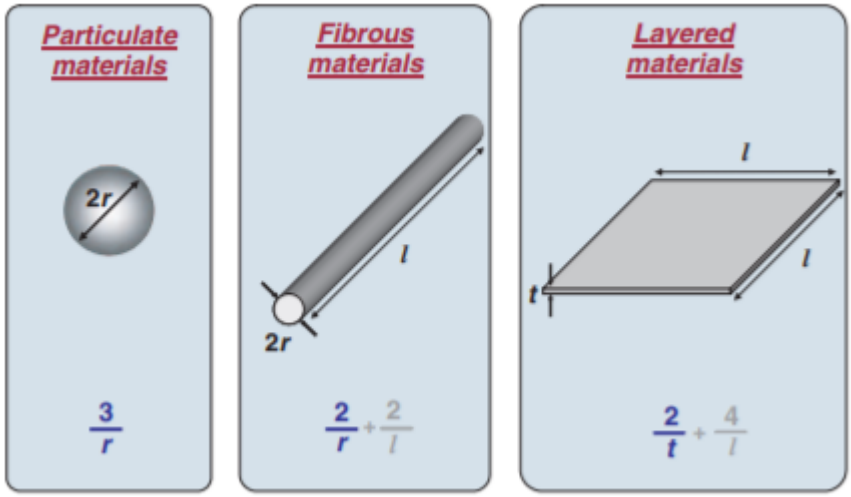

Figure 8: Composite reinforcement configurations [43]

properties that the composite system will display, and while orientation is important, volume fraction, or the quantity of reinforcers in relation to the matrix are just as important. Material properties, such as elastic modulus, are calculated as an average of the present phases' moduli based off of the volume fraction as shown below.

$$E_C = V_m E_m + V_f E_f \text{ [43]}$$

In the equation, $\boldsymbol{E_i}$ is the elastic modulus of the phase and $\boldsymbol{V_i}$ is its volume fraction. The subscripts ***c, m***, and ***f*** refer to the composite, matrix, and fiber phases, respectively. Thus, by knowing the properties of the constituent phases, composite properties may be estimated, theoretically. However, these calculations have underlying assumptions such as an equal strain condition between the two phases and appropriate adhesion between phases, which heavily depends on processing methods, and compatibility of the two phases. Adhesion of fibers in polymer matrix composites (PMCs) will be further discussed in the following section.

3.1 Polymer Matrix Composites

Any of the three engineering material classes (metals, ceramics, and polymers) may be improved with fillers (reinforcement particles). PET and natural fibers are the focus of this study, so polymer-matrix fiber reinforced composites will be discussed here. Polymer production entails a variety of processes such as extrusion, pultrusion, and molding [44]. Creating a successful polymer-matrix composite depends on the optimization of filler orientation and size as well as its adhesion with the matrix, so the production method used must fulfill these criteria. Naturally, the production process will affect the performance and properties of the composite. Understanding the properties and interaction between matrix and filler can help tailor the properties of the resulting composite. For example, the addition of fibers to a matrix may affect the intrinsic viscosity of the matrix and alter the processing conditions, which, if not properly understood can lead to an uneven distribution of fibers. Not understanding fiber-matrix interaction can lead to a detriment in mechanical properties since fibers are agglomerating and creating stress concentrators rather than points of reinforcement [44].

3.2 Natural Fiber-Reinforced Polymers (NFRPs)

Fiber reinforced polymers (FRP) have been in use since the 1940s, when glass fibers were embedded into polymeric resins due to their improved strength and stiffness while promoting a lower density. These composites have been used for a variety of applications ranging from construction to space exploration and air travel [45], [46], [47]. Recent years have seen a rise in the use of plant-based natural fiber-reinforced composites (NFRCs) from hemp, flax, jute, bananas, coconuts, wood and more [48], [49], [50], [51]. NFRCs are attractive because of their low density, low cost, biodegradability, and environmental friendliness [49], [52].

While composite properties depend on the individual properties of matrix and filler phases, the interfacial shear strength (IFSS), governed by adhesion between the two phases, plays an important role in the combined properties. Adhesion between the two phases is either physical, due to a decreased surface energy between the two surfaces, resulting in an interface, or they can be chemical, where bonds between the filler and matrix are a result of coupling agents [53]. Silane treatments of glass fibers is an example of chemical adhesion that promotes bonding in an *interphase* – a three-dimensional network of bonds between the filler and the matrix.

Surface modifications play a critical role in the success of NFRPs since many natural fibers, especially lignocellulosic ones, are hydrophilic while polymeric matrices are hydrophobic. Measures that have been taken to improve surface properties include chemical modifications with silane and alkali treatments, plasma treatments, electron beam irradiation, and acetylation [47], [54], [55], [56], [48], [57], [58]. Surface modifiers aim to strip natural fibers of their hydrophilic properties and make them more compatible to their hydrophobic thermoplastic matrices given that absorbing moisture may be detrimental to the matrix during processing [51]. This is especially true of polyester-based composites given that polyesters are hygroscopic and undergo degradation in the presence of moisture. PET is one such polyester that undergoes hydrolysis or molecular chain scission in the presence of moisture. As shown in **Figure 4**, the scission of PET fibers releases organic acids. These acids promote hydrolytic degradation of natural fibers, meaning that the integrity of the composite as a whole is diminished in the presence of moisture during processing. [46], [50]

3.2.1 Fiber Properties

Fiber length and orientation of discontinuous fibers are other parameters that play an important role in the benefit of the composite's properties. There exists a critical fiber length at

which the transfer of load from matrix to fiber changes behavior. The critical fiber length can be calculated based on the fiber's length and diameter as shown below. Fiber lengths below the critical length lead to fiber pullout because there is improper transfer of stress from the matrix to the composite, whereas a length much larger than the critical length is optimal for [46], [59]. At points where the fiber length is below the critical length, voids left from pullout form and become stress concentrators – weak points in the composite. While inorganic fibers can be manufactured to a certain length and oriented more easily, the manufacturing of natural fibers is anatomically limited by the source and environment from which the fiber is obtained. [48]

$$\frac{l_c}{d_f} = \frac{\sigma_f(\varepsilon_c)}{2\tau_{my}}$$

The critical aspect ratio equation shown above gives the behavior of fiber dimensions at which stress begins to be transferred to the midpoint of the fiber and not just the end points. Here, σ_f is the tensile stress carried by the fiber, τ_{my} is the shear stress, ε_c the tensile strain of the composite, d_f is the fiber's diameter, and l_c is the critical length of the fiber [59]. The critical aspect ratio in the equation above is a mathematical explanation of the factors that affect fiber behavior at specific points in the fiber's length.

Aside from fiber dimensions, distribution and orientation influence the anisotropic properties of composite materials. For example, when fibers have a preferred orientation and are a load is placed parallel to the fibers, improvements in strength are benefited most whereas placing the load perpendicular to the preferred orientation turns the fibers into weak points. [57] Here, instead of reinforcing strength, the fibers become defects in the matrix that remove strength in one orientation. Thus, in order for more uniform strength to be exhibited in multiple loading directions, fiber orientation must be randomly dispersed, which is typically the case in natural fiber composites.

Thus, while NFRPs are still being explored as environmentally friendly replacements for inorganic fiber composites, there are still hurdles to be overcome in terms of processing and compatibilization of the fiber and the matrix. This is especially true for interfacial interactions, but the slew of surface modifiers being investigated make the widespread use of NFRPs more likely in the near future, especially in the case of compounding filaments for additive manufacturing, which is to be discussed next.

Chapter 4: Additive Manufacturing

Additive manufacturing (AM) processes refer to a series of processing techniques that directly use computer data from CAD files to create a three-dimensional object on a layer-by-layer basis. AM is an umbrella term for processes such as selective laser sintering (SLS), laser chemical vapor deposition (LCVD), stereolithography apparatus (SLA), electron beam melting (EBM), laser engineered net shaping (LENS), and fused deposition modeling (FDM). [60], [61], [62] AM processes date back as far as 1860, when cameras were used to build 3D replicas of subjects and even topographical relief maps [63]. However, AM technology as it is known now is derived from a stereolithography apparatus (SLA), which was patented by Charles Hull in 1986. This used a laser beam to selectively polymerize photo-curable resin. [61] In recent years, AM applications have been incorporated in education, the aerospace and medical industries, and even enhanced tissue engineering. This became possible when the original patents on what became known as 3D printers expired in 2009 and Fused Deposition Modelling (FDM) became popularized [62], [61]. As such, the most widely used AM process often dubbed as 3D Printing is FDM.

4.1 Fused Deposition Modeling (FDM)

Fused Deposition Modeling, is a process that was developed and trademarked by Stratasys This AM technology is an extrusion process by which a solid monofilament of material is melted into a viscous form that is then pushed out through a nozzle [60]. This process is also known as fused filament fabrication (FFF) or material extrusion additive manufacturing (MEAM). Like Computer Numerical Control (CNC) where software is used to control the movement of a machine, the nozzle in an FDM machine is controlled by a universal file type common to all AM methods called a stereolithography file (.stl). In doing so, the combination of

extruded material moving along an XY plane creates a series of cross-sections that, when stacked on top of each other, create a three-dimensional object. As mentioned earlier, AM processes are controlled by CAD files that are run through a slicer program that convert the design created in a CAD software into a series of layers that can be interpreted by an FDM printer. [60] While all AM processes have in common that a three-dimensional part is created from layers stacked on top of each other, FDM differs in that it depends on the extrusion of a material (often a thermoplastic). To further understand the implications of this, an overview of extrusion processes and how they are used to process thermoplastics will be discussed.

4.1.1 Extrusion

Extrusion is a thermomechanical process in which a molten system that is under controlled temperature and pressure is fed into a die of a predetermined cross section. [63], [64], [65] This process may be continuous (either with a single or twin-screw extruder) or discontinuous as is the case in ram extruders. In industry, hot melt extrusion is the largest converter of plastics, as most plastics are extruded at some point in their production. [64] For the most part, extruders are composed of a feeding section, a screw driving unit, a single or twin-screw assembly within a heating barrel, and a die system, as shown in **Figure 9** [65], [66].

Continuous hot melt extrusion entails an integrated process of blending or premixing a plastic, drying it, feeding it to the extruder, drawing, shaping, and cooling all before any secondary treatments are introduced. The extrusion process is nearly the same for both single and twin-screw extruders. As seen in the aforementioned figure, both of these systems are composed of a drive system that is in charge of supplying enough torque to the screw assembly for a polymer to be processed; a feed hopper whose geometry is optimized to help automatize the flow of polymer resin (typically in pellet or powder form) into the screw; a barrel and screw assembly that provide shear to melt and convey the molten polymers into the final assembly – the die system, whose

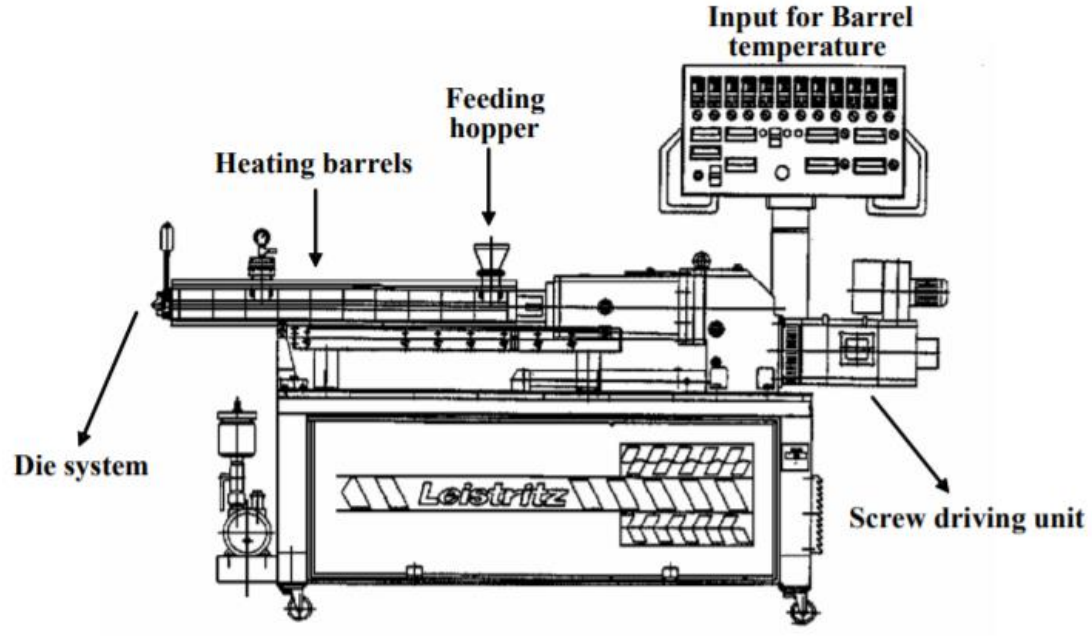

Figure 9: Hot-melt extrusion system [64]

orifice dictates the shape of the extrudate. [66], [67] As a result of the various assemblies in the process, the polymeric resin exhibits a change in behavior as it goes from resin to extrudate, especially within the heating barrels. Here, the resin, which is only transported by the screws up to this point, reaches a temperature above its T_g or T_m (depending on whether the system is amorphous or semi-crystalline, respectively) then it enters a state of viscous flow. This state of fluidity is induced mainly as a result of the shear friction produced between the barrel walls and the screws. [68], [69]

Like single-screw extruders, the above-mentioned steps take place in twin-screw assemblies as well. However, the first stage, in which the resin enters the screws may also be used for more consistent and better mixing than single-screw assemblies. This is due to the interaction between the parallel screws, as seen in **Figure 10**. Twin-screws have a series of kneading blocks that make uniform mixing of particles and powder more feasible than their single screw counterparts. Here, the rotational configuration of the screws also determines the effects imparted on the polymer being processed.

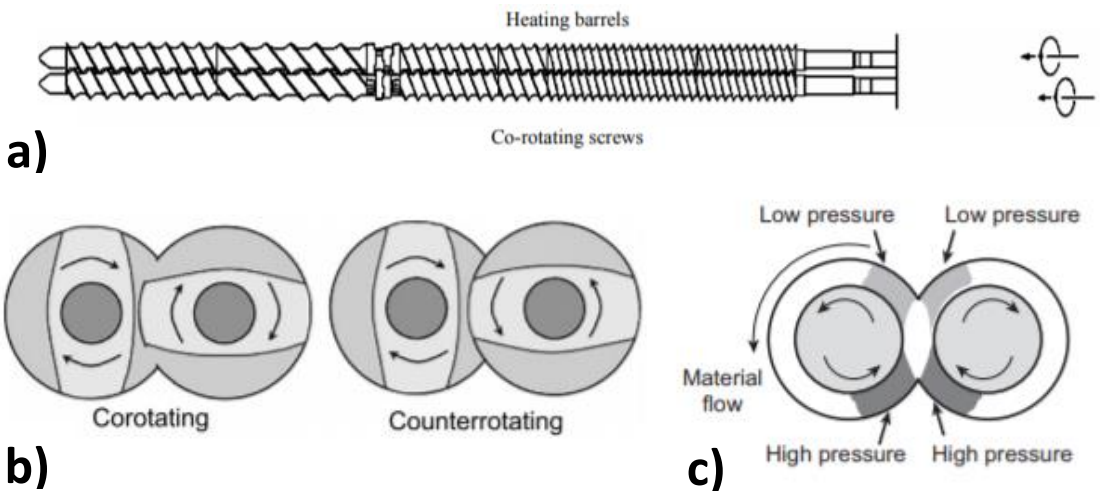

Figure 10: a) Twin-screw assembly [64] b) configurations and c) pressure distribution [86]

Given the uniform diameter of the die at the end of an extruder, a monofilament of a specific thickness and uniform cross section can be processed when the correct processing parameters are present. Thin monofilaments of plastic such as these are used as a feedstock for FDM printing. However, unlike extruders with screws to drive pellets forward, FDM printers have gears that drive the filament into the nozzle and into the (often heated) bed that will set the basis of the print.

4.2 Printing Direction – Mechanical Properties and Limitations

As previously mentioned, FDM (hereafter 3D printing) printing refers to the manufacturing technique in which a nozzle extrudes a viscous plastic made from a monofilament and onto a bed. When replicating the original CAD file, these stacked layers exhibit a stair step the size of the layer thickness. [60] Thus, there is a limited resolution to prints that is dependent upon the printer's ability to print thin layers.

Beyond the layer size and resolution that affects the interlayer bonding, the printing parameters also influence the mechanical properties of the print. For example, it has been shown that the raster pattern (the print direction and each successive layer's orientations) plays a role in

the isotropic qualities of a material. Since the beads extruded from the nozzle typically have a cylindrical shape, the layers do not sit flatly on top of each other and voids are inevitable sources of stress concentration, especially in load bearing specimens. [62], [70], [71] Thus, if 3D printing is to continue to grow as a manufacturing process, anisotropic effects must be either mitigated or exploited so long as the application can benefit from anisotropic behavior along one direction.

4.3 Potential for Composites

One final application of additive manufacturing, especially extrusion and 3D printing, is the ease with which materials can be compounded together – either resulting in polymeric blends or polymer matrix composites [72]. Recalling that twin-screw extruders have kneading zones and can be configured to optimize compatibility between polymers, it is not uncommon for them to be used to blend materials [73], [74], [75], [76], [77] Exploration of printable blends and composites is still under rapid expansion, but it promises to address problems in innovative ways.

Chapter 5: Materials & Methods

5.1 Materials

One way to take advantage of making new materials for 3D printing is to enhance recycling methods by exploiting plastic compatibility for compounding. In this case, recycled water bottles and cotton fibers from textile waste were combined into a natural fiber-reinforced polymer composite (NFRPC). Water bottles used as the polymer matrix for the composite were donated by Cordova Distributing Company, where the bottles did not meet quality control standards and were to be discarded (Cordova Distributing Company, LLC, El Paso, TX, USA). To maintain uniformity in the matrix, the tops of the bottles were separated and only the body was used. Two types of denim cloths were used to investigate the effect of indigo dyes on mechanical behavior. The first were white twill-jean cleaning cloths from Ted Pella, Inc (Ted Pella Inc, Redding, CA, USA) while the indigo-dyed cloth came from post-consumer Guess-brand jeans (100% cotton). The latter represented textile waste that was not bleached to remove dyes before processing. Chemicals used in the functionalization of the fabrics including sulfuric acid (98%), hydrochloric acid (36%), and (3-Aminopropyl)triethoxysilane (hereafter APTS) 98% were obtained from Sigma-Aldrich (Sigma-Aldrich, Inc, St. Louis, MO, USA). Arm & Hammer ™ baking soda (sodium bicarbonate) was also used to neutralize fibers after hydrolysis (Arm & Hammer, USA).

5.2 Procedures

Developing the composite filament was achieved through the following steps: extruding the PET matrix alone, obtaining cotton fibers from denim cloth, hydrolyzing and functionalizing the fibers, and then extruding the composite. In doing so, the first obstacle came from properly and uniformly shredding the bottles into pellet-sized dimensions. Initially, the bottles were

introduced to a Filabot Industrial Reclaimer (Filabot, Barre, VT, USA) in the as-received condition, which led to an accumulation of large bottle flakes on the inner wall of the reclaimer. In an attempt to mitigate this, a Carver hot press (Carver, Inc. Wabash, IN) was used to flatten the bottles in longitudinal direction, making it easier to shred a larger volume of bottles within the reclaimer at once.

The initial extrusion attempt used hot-pressed bottle flakes and a Filabot EX2 filament extruder with the accompanying Filabot Airpath cooling system. The particles retrieved from the reclaimer varied in size from flakes up to 1cm large to a very fine powder. To promote uniformity, these were sieved with a 1mm mesh sieve. The powder and flakes were then kept separate. Since flakes were the predominant size of recovered particles, these were used in the first extrusion attempt.

Despite attempts to extrude at 260^{o}C, temperatures suggested in literature [78]**,** [76] the material was not viscous enough to form a consistent filament and a very thin spool was collected (shown in **Figure 11a**). Salmien Pontus suggests that the presence of moisture before thermally processing the recycled PET (through hot pressing or extruding) leads to a process of hydrolysis that breaks de-polymerizes the molecules and drops the intrinsic viscosity of the material [79]. Considering that the bottles were pressed between two metal plates heated to 130^{o}C, it was hypothesized that hydrolysis was indeed occurring even before the bottles were processed through the reclaimer. To prove this, rheological tests with a melt flow indexer were conducted on flakes that were hot-pressed and others that were processed without hot-pressing. The flakes for the latter were obtained by first flattening the bottles manually as much as possible, then reclaiming and sieving them. Upon first look, it was evident that a chemical

change had occurred in the flakes that were hot-pressed (HP) because there was a significant color difference between these and non-hot-pressed (NHP) (**Figure 11b**).

Figure 11: a) First attempt at extruding recycled PET (RPET) with air cooling b) Comparison of 1) HP and 2) NHP RPET

5.2.1 Melt Flow Index (MFI)

A comparison of rheological properties between hot-pressed recycled PET (HP RPET) and non-hot-pressed PET (NHP RPET) was conducted in a Tinius Olsen MP1200 Melt Flow Indexer before attempting another extrusion. As per ASTM D1238-04 standards, each PET state was tested three times at 250^{o}C with an added 2.16kg weight to provide constant shear and promote flow during the test. [80]. The results of this test are seen in **Figure 12** and **Table 1**. Average melt flow indexes of 69.06 ± 9.89 g/10 min and 76.27 ± 29.71 g/10 min were recorded for NHP and HP PET, respectively. The difference between both MFI values was significant enough to show a difference in viscous properties while extruding. Thus, from this point forward, it was determined that NHP PET was a better material for extrusions, given that the viscosity would allow it to draw into a monofilament of a somewhat regular size.

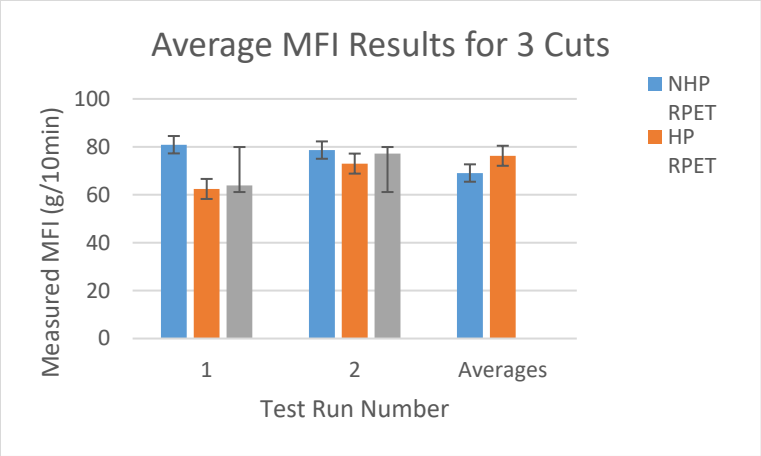

Figure 12: HP vs. NHP MFI results

Table 1: Average measured MFI (HP vs. NHP)

Material Condition (RPET)	HP	NHP
Average MFI (g/10min)	76.27	69.06
Standard Deviation (±)	29.71	9.89
Coef. of Variation (%)	38.96	14.32

5.2.2 RPET Extrusions

Following the MFI tests, the process of shredding the PET bottles was improved to remove the need for sieving. To do so, a Fellowes 99Ms Micro-Cut Shredder was used. Since the bottles could not be introduced as-received into the shredder, they were first cut into strips that fit the shredder's slit. First, the bottleneck and base were removed so that only a hollow cylinder remained. This was then cut along the longitudinal axis into six to eight even strips that fit into the shredder's slit. Shredding only with a cross shredder resulted in thin, confetti-like strips that easily tangled and prevented continuous feeding within a hopper, so these were introduced (along with the previously removed top and bottom of the bottle) into the Filabot Reclaimer once more. Unlike previous runs through the reclaimer, processing through the shredder led to a more uniform particle size that needed little to no sieving. These particles were then dried for five hours at 150^{o}C in a compressed air dryer (Dri-Air DFAM Micro-Dryer, East Windsor, Connecticu, USA). The resulting pellet-like particles were extruded using a twin-screw extruder (Model ZK 25 T, Dr Collin GmbH, Ebersberg, Germany) to obtain a uniform filament with a 1.75 mm diameter. Extrusion parameters are seen in **Table 2**. The filament was water cooled in a room temperature bath of distilled water. The resulting filament (**Figure 13**) served as the

source for printing a control group of both DMA and impact strength specimens out of pure recycled PET (RPET).

Table 2: RPET extrusion parameters

Zone	Zone 1	Zone 2	Zone 3	Zone 4	Zone 5	Zone 6	Pressure 1 (bar)	Extruder Screws	Melt Pump Screws	Melt Pump Pressure	Feed Rate
Value (unit)	200 (°C)	240 (°C)	260 (°C)	260 (°C)	240 (°C)	220 (°C)	66 (bar)	38-43 (rpm)	12 (rpm)	106-108 (bar)	9 (%)

5.2.2.1 Cotton Fiber Retrieval

The development of the composite (both with white denim and indigo denim) relied on the ability to obtain fibers small enough to reinforce the 1.75 mm filament. This task was achieved with two simple tools and a very tedious process. In the absence of a cutting mill, cloth shredding was done manually with the help of a wire brush and a ceramic tile. The tile served to provide a surface hard enough to artificially wear the cloth with the brush.

Figure 13: RPET 1.75mm filament

For the white denim samples, a square cloth with dimensions of 6in by 6in was screwed onto a small wooden block that was easy to handle in one hand to hold the cloth in one place as it was brushed on the tile. Brushing occurred in the direction away from the wooden block to uniformly wear down the cloth and release small fibers. Fibers noticeably accumulated between the bristles of the brush and on the tile surface, where they were retrieved and placed on an aluminum pan that kept them in place (due to their light weight, they easily move about if not secured).

The same brushing process was reproduced with the post-consumer denim pants shown in **Figure 14**. However, unlike the white denim cloth, which came in a predetermined size, a small piece had to be cut off from the pants and the stitches adjoining the material had to be removed. For the proof of concept conducted in this study, only a section of the pants was used. Given the compounding percentages used in this study (10 vol % cotton, 90% RPET), one single pair of pants can serve as reinforcement for a large amount of PET-cotton composite filament.

Figure 14: Post-consumer denim pant processing

After brushing, the resulting fibers take a form that looks like lint with some lingering yarn strings. For the most part, the largest strings were removed, but any strings that were frayed

or showed potential for breaking down further were left within the bulk of fibers given that the functionalization treatment would further break down the fibers.

5.2.2.2 Cotton Functionalization

Functionalization refers to the preparation of the reinforcing polymer fibers for being incorporated into the matrix. Thus, the chains of the cotton had to be chemically altered to facilitate acceptance of new side chains. To do so, both types of cotton fibers were introduced to a series of chemical treatments based on a procedure by Araújo [75], who created a similar reinforcement with cotton and PLA. In this process, 10 grams of cotton fibers were exposed to an acid hydrolysis. The fibers were submerged in an acid solution containing 180mL of distilled water, 20mL of 98% H_2SO_4 and 200mL of 36% HCl and stirred for 150minutes at 40^oC. [75] From here, the suspension containing the fibers and solution were filtered using a vacuum filter and a Grade 5 Qualitative Filter Paper (GE Healthcare Life Sciences) until no liquid is left. The damp fibers are then placed in a beaker where a solution of 5% sodium bicarbonate is added until neutral. At this point, the suspension was washed in distilled water for 24 hours before drying in a VWR Forced Air Oven (VWR International, Radnor, PA, USA) for 48 hours. When dry, the suspension was removed from the oven and prepared to undergo the same acid hydrolysis process once more before being prepared for silanization – the functionalization of fibers through submersion in a silane.

Silanization is a very similar process to acid hydrolysis, but the submersion media changes. In this case, 1 gram of (3-aminopropyl)triethoxysilane (APTS) was added to a 500 mL solution of 90% vol ethanol to water . Once the cotton was added to the solution, the mixture was stirred for another 24 hours at 60^oC, after which it was dried for 7 hours at 80^oC. The resulting dry fibers showed some discoloration (the white fibers turned brown), but the large strings were

indistinguishable from the rest of the agglomerated mass of fibers that were then mixed in the extruder. Indigo dyed fibers underwent the same functionalization treatments, but they did not exhibit any changes in color, which suggest that the indigo was doing something to the chemical interactions between PET and the cellulose from cotton.

5.2.2.3 Composite Extrusion

Much like the first attempt at extrusion, the pellet-like shredded PET bottles were first dried at 150^{o}C for five hours. Then, the fibers and pellets were mixed thoroughly in a beaker to give a 10 vol % cotton-PET mixture. In this case, 100mL of functionalized fibers were mixed with 900mL of PET flakes (**Figure 15**). The homogeneity of the mixture shown allows for a uniform distribution of fibers once extruded.

Despite twin-screw extruders being more useful when mixing polymers, the amount of the mixture was small enough where a single screw extruder was more favorable. Thus, using the setup in **Figure 16**, a Filabot EX2 single-screw extruder was used at 250^{o}C and a screw speed at the highest possible value (slowly building up to it as pressure became uniform in the barrel). A 1.75mm ± 15mm diameter filament resulted, as shown in **Figure 17a**.

Figure 15: RPET-10 vol% white cotton mixture

Figure 16: Filabot EX2 extrusion setup

Figure 17: 1.75mm composite filaments - a) RPET-10 vol% WC and b) RPET-10 vol% IC

The same process was repeated for the indigo-dyed fibers. The only feasible difference came from the condition of the fibers after they were functionalized. Originally, the white denim fibers were much thinner due to successful hydrolysis, but the presence of indigo on these fibers prevented full hydrolysis. As a result, larger fibers were still present and mixing became more difficult because the fibers adhered to one another, so the extrusion temperature was raised to 260^{o}C. Improper mixing caused visible agglomeration in the resulting monofilament, which yielded an inconsistent filament diameter. The resulting filament of 1.75mm ± .25mm is shown

in **Figure 17b**. It should be noted that the indigo dye remained present in the filament as its color is clearly derived from this dye.

5.2.3 Printing Test Specimens

With the three filaments ready to go, the next step in evaluating their mechanical properties and effects of compounding was to print specimens. To combat hygroscopic degradation within the filaments and because they were all water-cooled, they were all set to dry at 80ºC for five hours. Due to limitations with time and available equipment, this study focuses on impact specimens, dynamic mechanical analysis (DMA), and fractography performed through scanning electron microscopy (SEM).

Specimens printed for DMA and impact tests were all printed with a Prusa i3 MK3S printer and a crosshatched raster pattern of ± 45º to the longitudinal axis of the specimen (Prusa Research, Czech Republic). All prints were completed at 260ºC at a relatively slow speed of 30 mm/s. DMA specimens had an infill density of 100% while impact specimens were only filled up to 50% due to limitations in printable material. Representative DMA prints for each of the filaments are shown in **Figure 18**. The indigo-cotton specimen has a lower print quality because agglomerations in the filament led to inconsistent diameters that caused the printer nozzle to clog and print inconsistently.

In an attempt to improve printing with this material, it was decided that the indigo-cotton filament should be pelletized in a Dr. Collin Strand Pelletizer and re-extruded in the Collin twin-screw extruder to homogenize mixing of the fibers and normalize the diameter of the filament. Doing this with only about 250g of material introduced two risks: one of running out of material before stabilizing the filament diameter, and another degrading the material further when exposing it to an extra thermomechanical process. Actions were taken once more to mitigate

hygroscopic degradation by drying the pellets at 150°C for 5 hours before attempting to extrude. The extrusion process exhibited much better homogenization as the extrudate was dyed a deep navy blue with a chrome-like finish coming from the uniform distribution of fibers. Drawing this into a filament was a challenge since the melt pump was removed because it had clogged the extruder previously.

Table 3:Extrusion parameters for indigo cotton in the Collin extruder

Zone	**Zone 1**	**Zone 2**	**Zone 3**	**Zone 4**	**Zone 5**	**Zone 6**	**Pressure 1**	**Extruder Screws**	**Feed Rate**
Value (unit)	200 (°C)	240 (°C)	260 (°C)	260 (°C)	240 (°C)	220 (°C)	66 (bar)	50 (rpm)	9 (%)

As material began to stabilize, the belt take-off used to continuously pull the extrudate stopped working, which in turn allowed extrudate to accumulate into a ball and even foam in some sections. In an improvised attempt to continue processing, the Filabot EX2's accompanying filament spooler was used. Unfortunately, this was not done quickly enough to continue processing, and all of the prepared material had been rendered unusable after exiting the extruder. Re-pelletizing was no longer an option either because of foaming or because the resulting geometry was not compatible with the pelletizer.

While the re-extrusion attempt was a failure, it did show that extruding indigo-cotton with a twin-screw extruder was possible when enough material was present, and it mixed the components better. Furthermore, while the inability to print at the time of publishing means that obtaining mechanical properties for this composite are not possible, its filament structure was studied under the microscope to compare the adhesion of fibers to the matrix and compare it to the white-cotton composite.

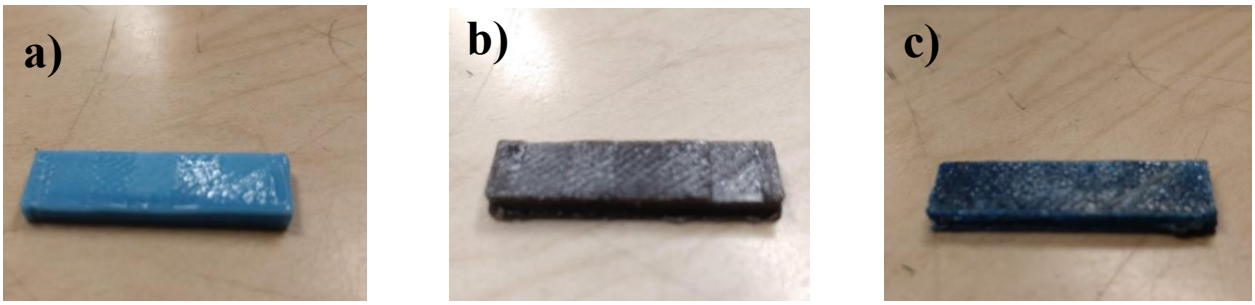

Figure 18: Representative DMA specimens for a) RPET b) RPET-WC and c) RPET-IC

5.2.4 Attenuated Total Reflectance (ATR)

Composite constituents were identified through attenuated total reflectance (ATR) analysis using a Nicolet iS5 FTIR Spectrometer with an iD7 ATR Diamond accessory (Thermo Fisher Scientific, Waltham MA, USA). The scan was observed from 400 to 4000 cm^{-1} on monofilaments of RPET, RPET 10 vol% white denim (RPET WC), and RPET 10 vol% indigo denim (RPET IC) as well as on a piece of white denim fabric for comparison. Furthermore, because of the differences in color present in the final extrusion of the indigo cotton composite, two spectra were retrieved to check for any differences. A homogeneously mixed translucent piece of filament (labeled RPET-IC Dark) and a lighter colored foamed piece of filament (RPET-IC Foam) were analyzed.

5.2.5 Dynamic Mechanical Analysis (DMA)

Dynamic mechanical analysis (DMA) was performed on a Perkin Elmer DMA (PerkinElmer Waltham, MA, USA). Printed specimens for this had the following dimensions: a length of 30mm, width of 9mm and thickness of 3mm. A temperature scan was carried out in dual cantilever at a frequency of 1 Hz and dynamic force of 2N from 25^{o}C to 105^{o}C at a rate of 5^{o}/min. The range of the scan was chosen arbitrarily around the reported glass transition

temperature (T_g) for PET of 67°C for amorphous PET and 81°C for crystalline PET [81]. PerkinElmer Pyris ™ software was used to analyze the information given by the DMA. The same conditions were attempted for all three types of specimens. However, due to the poor quality of the RPET-IC specimen, the instrument could not get a proper read and DMA could not be performed on this composite.

5.2.6 Impact Test

Izod pendulum impact resistance tests were carried out on five specimens of each RPET and RPET-white-cotton composites (RPET WC). ASTM D256-10 specimen dimensions were used with a cross-hatched raster pattern and the notch printed on top of the specimen, as proven by Roberson et al to be the most effective way to mimic a manufactured notch ([82],[62]). A Tinius Olsen IT 504 polymeric impact testing machine was used to measure impact resistance (J/m), impact strength (J/m^2) and break energy (J) (Tinius Olsen, Horsham, PA, USA). Test were conducted with a drop height of 609.6 mm for a 15J pendulum capacity and an impact velocity of 3.46m/s. It should be noted here that the specimens used for this were printed with a 50% infill to conserve material.

5.2.7 Fractography (SEM)

In order to understand how well the cotton fibers adhered to the PET matrix and to understand their behavior upon failure, filament sections and impact facture surfaces were looked at under a Hitachi SU3500 SEM (Hitachi High Technologies America, Irving, TX, USA). Due to the non-conductive nature of the polymeric surfaces, electron charging occurs under complete vacuum, thus the SEM was used in variable pressure mode at 60 Pa to prevent charging. An accelerating voltage of 15kV was used in UVD (Ultra Variable-Pressure Detector) mode.

For a representative surface to be seen, the filaments used were pulled in tension until failure and both ends were viewed, along with a look at the transverse axis of the filament. This was done for all three filaments (RPET, RPET WC, and RPET IC). However, because of the failed extrusion of the indigo-cotton composite (RPET IC), three different sections of filament were seen. These were identified as a translucent one that had more time in the barrel, which looked darker than the others, a lighter translucent one and one that foamed. All three were observed to understand how well the fibers adhered to the matrix and what kind of reactions may have led to the foaming.

Fractography was conducted on representative impact specimens that most closely resembled the average values of the test set. As will be seen in the next chapter, most of the specimens fractured completely after the test, so they had a fracture surface that could be analyzed to understand the behavior of crack propagation in these composites. Furthermore, poor adhesion to the matrix in the form of pullout could be identified, as well as a fiber length, as will be discussed further below.

Chapter 6: Results & Discussion

6.1 Melt Flow Index

Recalling that MFI gives an idea of intrinsic viscosity of a polymer system, it is also indicative of the state of degradation that polymer chains exhibit. In fact, it was first used to quantify how hot pressing the water bottles before extruding was detrimental to the latter stages of processing the filament. On another note, this same instrument was used as an indicator of how the cellulose fibers were affecting the matrix. As seen in **Table 6.1**, the baseline material, RPET, had the lowest MFI at 69.06 ± 9.892 g/10 min. Both composite materials exhibited much higher melt flow rates, indicating a plasticizing effect from the cotton fibers. This was especially true of white denim fibers, which yielded an MFI of 147.707 ± 33.831 g/10 min whereas indigo fibers yielded 92.404 ± 15.424 g/10 min. The difference in composite flow rates could be due to two reasons: 1) the hydrolysis process was incomplete for indigo fibers and agglomeration increased resistance to flow (hence, a lower MFI) and 2) the presence of indigo, which does not degrade at the temperatures used, interfered with molecular chain movement and lowered the MFI. Furthermore, the change in color for white cotton after hydrolysis, which was absent in indigo cotton, left larger fibers even after extrusion.

Table 4: MFI results for all three filaments

Material	MFI (g/10min)
RPET	69.06 ± 9.892
RPET 10% WC	147.707 ± 33.831
RPET 10% IC	92.404 ± 15.424

6.2 Attenuated Total Reflectance (ATR)

Attenuated total reflectance (ATR) was used to identify any chemical changes to the matrix or fibers induced by the compounding process. As seen in **Figure 19**, save for a few outlying peaks, RPET and its composites exhibit nearly identical spectra, which is expected given that

RPET is the main component. Two spectra were collected for indigo cotton (IC) because of a translucent and foamed section of filament that were produced, as explained in the previous chapter. One notable difference between RPET and both composites is evident at 1775 and 833 cm^{-1}, two peaks that are largely suppressed in the composites, indicating a change to the RPET matrix is happening while compounding. The presence of cellulose in both composites (IC and WC) is identified by the peaks between 2800 and 3000 cm^{-1} for the RPET_WC and both RPET_IC spectra [75]. Furthermore, all cotton-containing filaments exhibit peaks representative of silane functional groups at 1575 cm^{-1} from successful functionalization, even in the indigo state. A peak at 1540 cm^{-1} and two in the range of 1150-1200 cm^{-1} are only present for the RPET while the composites and denim alone all flatline as well. At 1175 cm^{-1} (seen more closely in **FIG**), the composites all exhibit a peak representative of silanization as neither the denim sheet nor RPET have this peak. This peak is indicative of new bonds created by the functionalization in all composite variants. Evidently, the functionalization process successfully created new bonds within the composite filaments and even changed the RPET matrix in some cases, an early sign of adhesive bonding between the matrix and fiber that will be further explored with other methods.

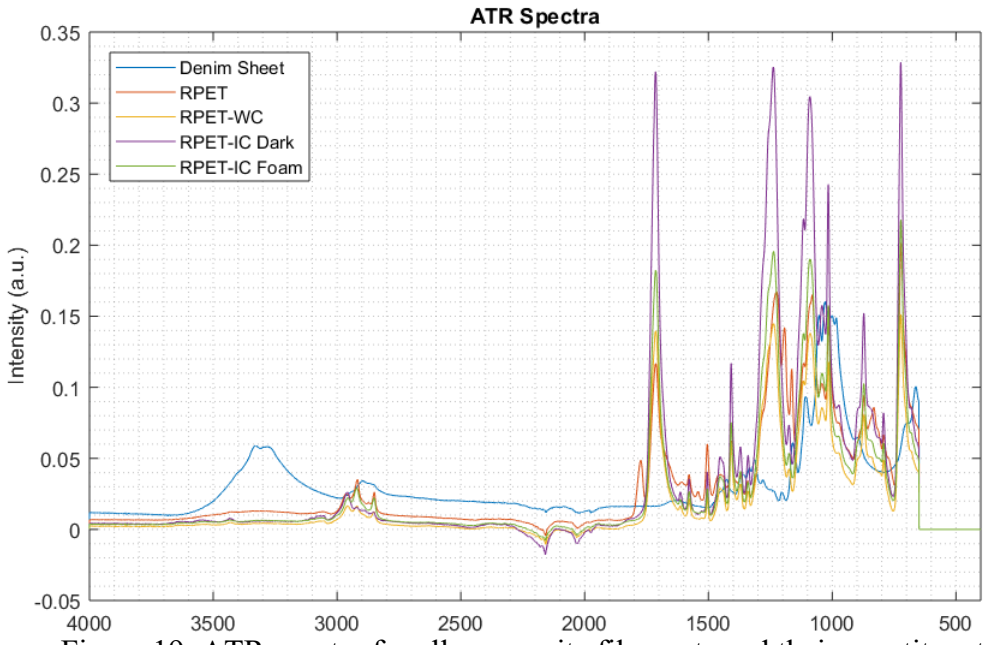

Figure 19: ATR spectra for all composite filaments and their constituents

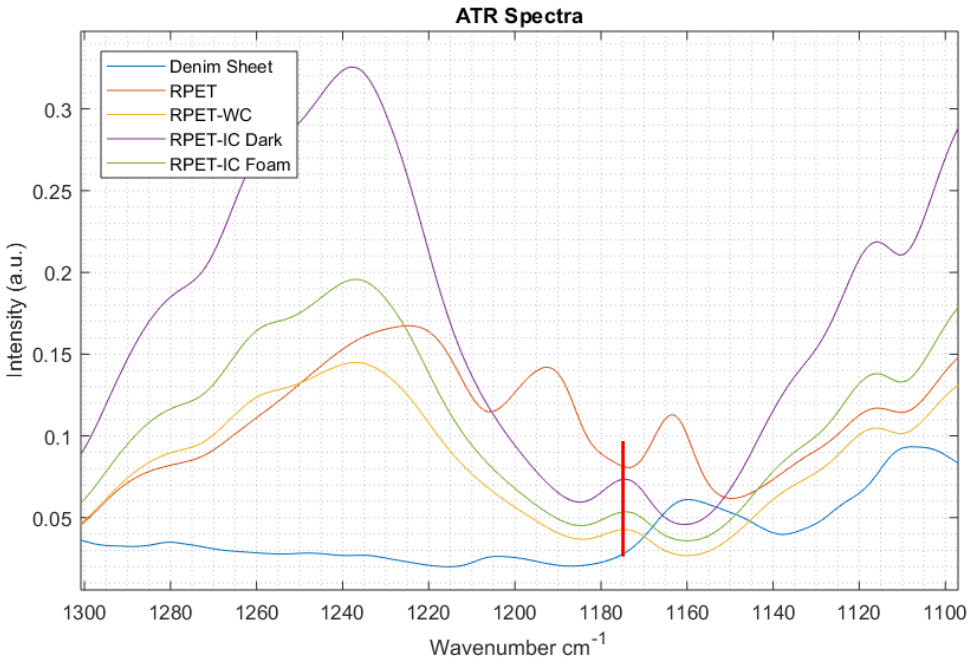

Figure 20: Shortened section of the ATR spectra to point out the presence of a new peak (red bar) in the composite materials.

6.3 Dynamic Mechanical Analysis

DMA temperature scans for RPET and RPET-WC were completed on three specimens of each. The average values for glassy onset based on storage modulus drops and the max tan delta are presented in **Table 5** while representative curves of these are seen in **Figure 21**. As can be seen in the table, the value of storage moduli at the onset of a transition were relatively close at 64.59 GPa ± 45.159 GPa and 65.81 ± 33.955 GPa for RPET and RPET-WC, respectively. Both onset values are relatively close, indicating no big change. However, there was a slight drop in temperature from 78.59ºC to 77.40ºC once the cotton fibers were added, suggesting a plasticizing effect. This was not a complete shift to the left, though. The temperature at which the tan δ curve was greatest increased with cotton, going from 86.99ºC to 89.18ºC. Overall, this creates a widening of the transition from glassy to rubbery behavior, giving a larger range of temperatures between which thermal processing can occur. Finally, the max tan δ value at these

points increased from 0.28 to 1.34. The increase in tan δ, also known as damping, suggests that the material will have a better damping capacity, often associated with a better dissipation of energy, or impact resistance at the expense of elasticity [83], [84]. Whether or not this is true is discussed in the next section.

Table 5: Summary of DMA findings for RPET and RPET-WC

	Storage Modulus		Loss Tangent	
Material	**Glassy Onset (Pa)**	**Temperature (°C)**	**Max Tan δ**	**Temperature (°C)**
RPET	6.46E+10	78.59	0.28	86.99
RPET 10% WC	6.58E+10	77.40	1.34	89.18

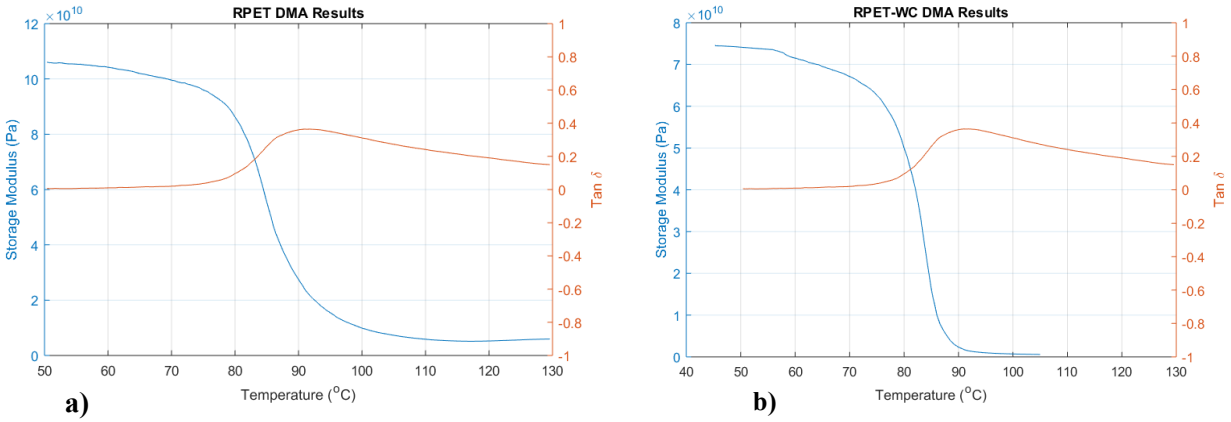

Figure 21: Representative DMA curves for a) RPET and b) RPET-WC

6.4 Izod Impact Tests

Five impact tests were completed for each of the printable filament states, meaning that only RPET-IC was not tested. The average values of these tests are shown in **Table 6**. As expected from the DMA results, a toughening effect is evident in the cotton specimens given that the impact resistance and impact strength were increased from 14.4 ± 2.58 J/m to 23.3 ± 5.21 J/m and 1380 ± 245 J/m^2 to 2270 ± 501 J/m^2, respectively. The higher energy needed to break the specimens is indicative of more ductile behavior that dissipates impacts better. In other words, the addition of functionalized cotton fibers is toughening or even plasticizing the RPET matrix. It

is worth mentioning as well, that, while RPET fractured completely in a brittle manner, the increased ductility of adding cotton led to incomplete fracture of two of the specimens. Here, the upper half of the specimen was left hanging even after impact (a microscopic version of this is seen in **Figure 24**). Recalling that fiber orientation affects mechanical properties, it is possible that the, because the beads are drawn in one direction, the fibers align with printing direction. Since these specimens were printed in a cross-hatched raster patter, the fiber reinforcement thus has a similar weave improving toughness. SEM images of representative fracture surfaces for each material support this hypothesis.

Table 6: Average impact test results for RPET and PRET-WC

Material	Impact Resistance (J/m)	Impact Strength (J/m^2)	Impact Break Energy (J)
RPET	14.38 ± 2.579	1384 ± 243.988	0.1792 ± 0.033
RPET-WC	23.3 ± 5.210	2268 ± 501.318	0.2872 ± .064

Figure 22a shows the fracture surface near the v-notch interface. At the interface, interlayer adhesion is clear as the individual beads are indistinguishable, unlike those seen in the following layers **Figure 22b**. Since these samples were printed at 50% infill, interlayer bonding did not homogenize the structure and the individual layers are distinguishable. In the image, this results in multiple fracture surfaces being seen rather than just one. Within these surfaces, smooth “mirror” sections abound near hackle lines, where fracture planes give rise to lined patterns.

On the other hand, **Figure 24a** shows a similar image near the v-notch interface of the white cotton representative specimen. Despite having the same printing parameters, the beads with cotton fiber appear to be thinner with a roughness to the surface due to the integration of cellulose fibers in the matrix. **Figure 24b** shows that large mirror sections are still present with a distinct mist and hackle regions transitioning into the fracture along the propagation of the crack.

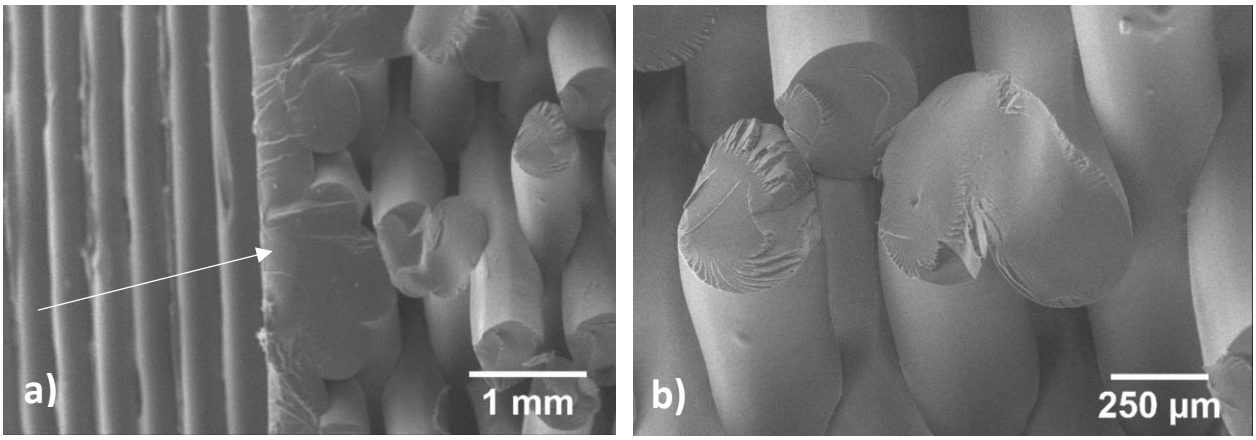

Figure 22: Representative RPET fracture surface near the v-notch at a) low magnification and b) high magnification

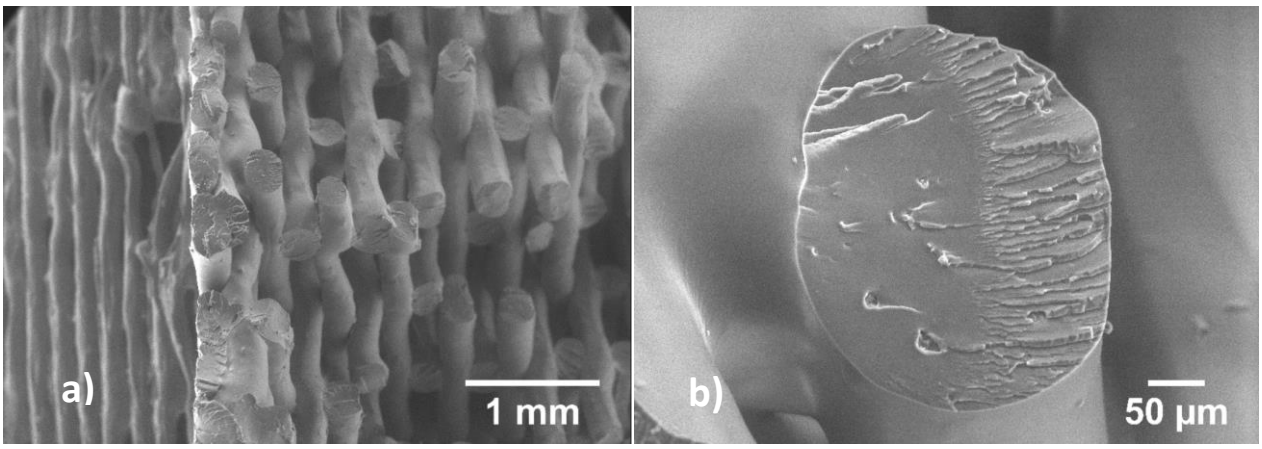

Figure 23: Representative RPET-WC fracture surface near the v-notch at a) low magnification and b) high magnification

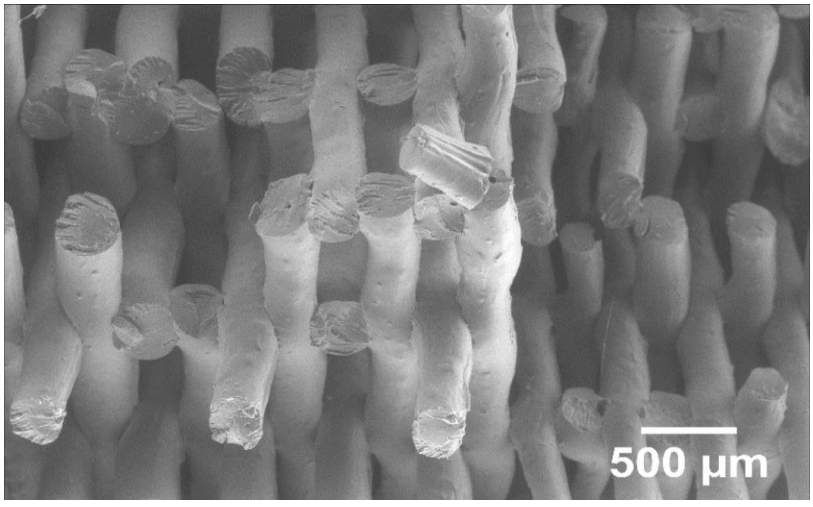

Figure 24: RPET-WC hinge fracture

However, unlike the mainly smooth surfaces of RPET impact specimens, those from RPET-WC have regions where the cotton fibers helped resist the impact. Despite the shear deformation zones surrounding the fibers, there are no voids present, indicating that proper adhesion between the matrix and fibers occurred and energy dissipation is taking place. The larger deformation present in the RPET-WC specimens concurs with the impact and DMA results discussed thus far. Below, the filaments of each of the composites are discussed to further enlighten about the behavior of each variation in the absence of complete mechanical analyses.

6.5 Scanning Electron Microscopy (SEM)

Small filament sections of all three composite variants were pulled along the longitudinal axis to create a fracture surface indicative of the material's response to tension. **Figure 25** depicts such a fracture surface for the RPET filament. The solid arrows demarcate a smooth "mirror" surface where little to no deformation took place. Continuing the crack propagation in a counterclockwise direction for **Figure 25a** and a clockwise one for **Figure 25b**, the smooth areas are replaced with small mist planes that lead directly to hackle planes that ultimately led to fracture. The relative absence of plastic deformation are signs of a material that does not deform easily and therefore fractures in a brittle manner.

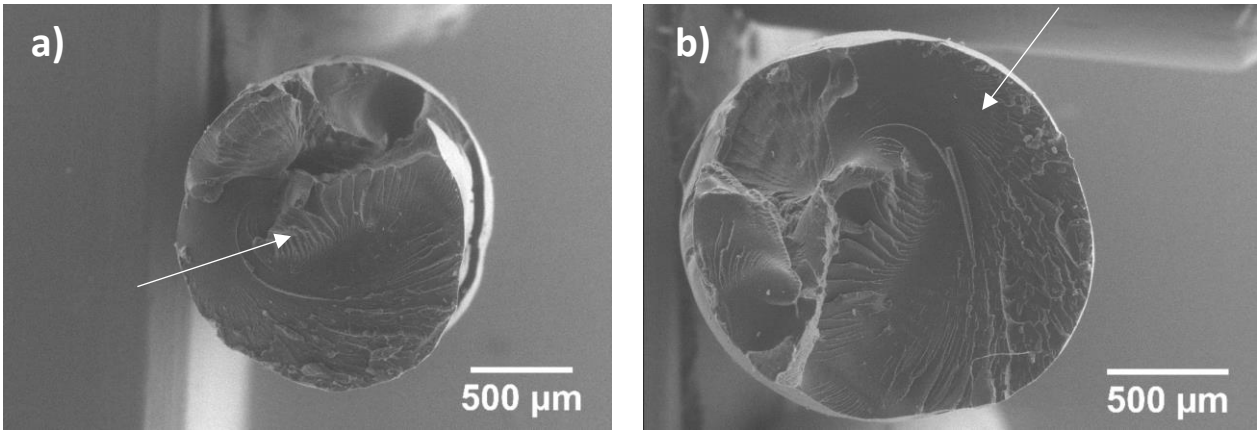

Figure 25: RPET filament fracture surfaces

Once white cotton fibers were added to the matrix, there was a different response to stress and the fracture surface changed significantly. Unlike RPET, RPET-WC underwent significant plastic deformation, Error! Reference source not found.. The top section of both images demonstrates extensive plastic deformation surrounding small circular artifacts (circled in the figure) that likely occurred with the pullout of fibers below the critical aspect ratio. The lower part, on the other hand, shows much larger voids resulting from strain fields formed while deforming. Evidence that it was not formed by poor adhesion is the size of the void when compared to a fiber as well as the fact that both sides of the fracture surface contain matching sections of these voids. Overall, the composite shows appropriate adhesion. The fibers seen on the surface of the filament are properly incorporated into the matrix and there is no significant evidence to show that poor adhesion caused the fracture. In fact, the fibers pointed out by the arrows are all properly adhered to the matrix as there are no voids surrounding them.

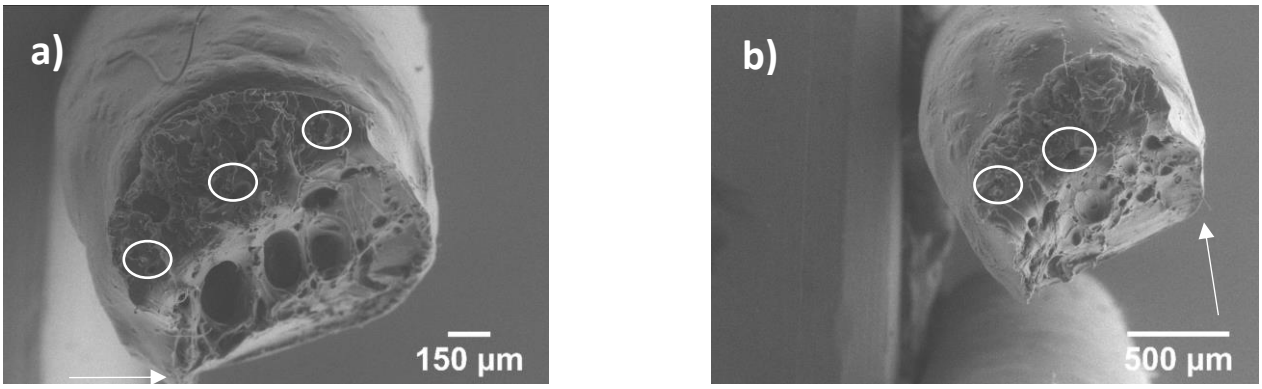

Figure 26: Low magnification RPET-WC a) top and b) bottom fracture surfaces

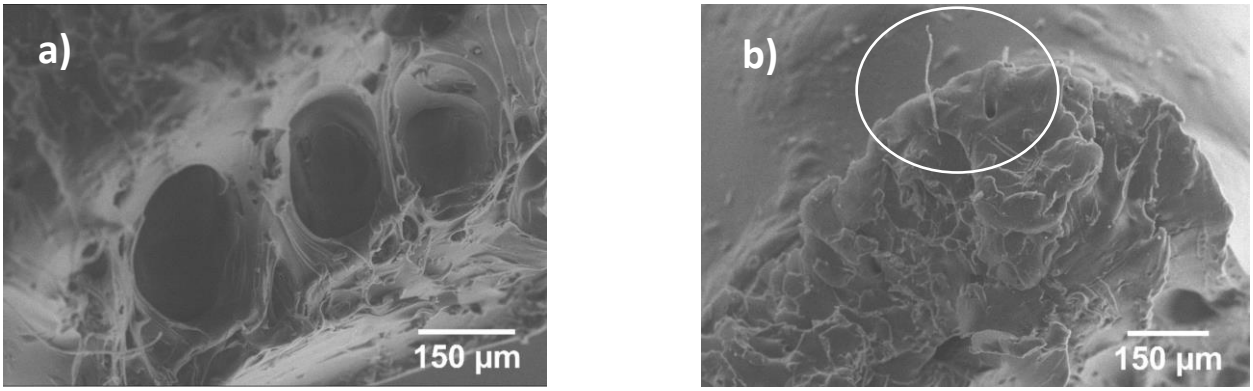

Figure 27: High magnification RPET-WC a) top and b) bottom fracture surfaces

Higher magnification images of the same fracture surfaces are shown in **Figure 27**. **Figure 27a** is a closeup of the strain fields, which shows the bottom of the pit. The absence of fibers within the voids and extensive deformation surrounding them further drives the point that these are strain fields that were not caused by the fibers. The deformed region surrounding the voids even depicts the localized plastic deformation of regions known crazing. Unlike the RPET filament, this filament exhibits highly ductile behavior, which is also depicted in **Figure 27b**. The multiple fracture planes and white edges are all results of plastic deformation as well. The top section within the circle shows a fiber that was exposed by the fracture surface and a void left behind from fiber pullout right next to it. The instance of fiber pullout is proof that stress was properly transferred to the fiber from the matrix in deformation, but the interface between the two was weaker than the stress that the fiber was experiencing whereas the section where the fiber had good enough adhesion to remain in place.

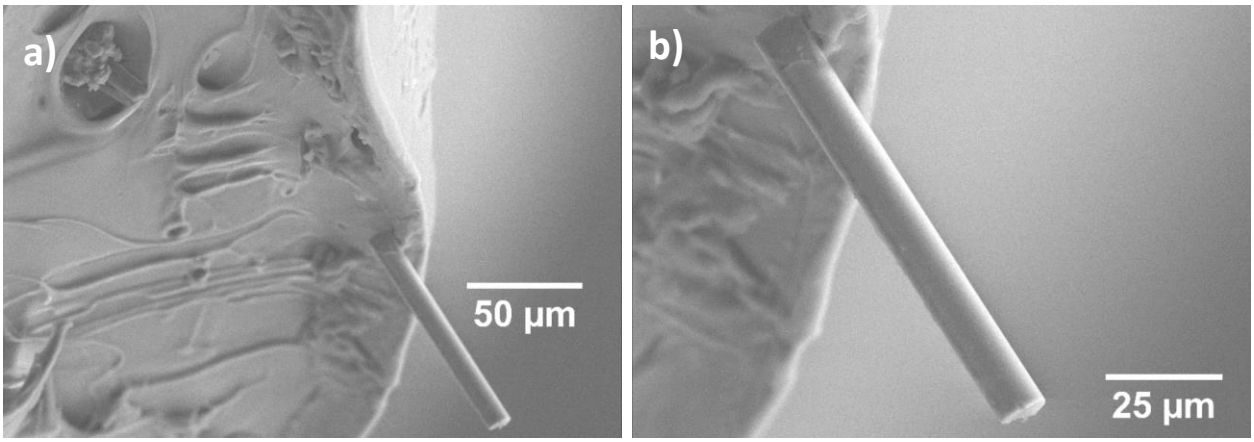

Figure 28: High magnification RPET-WC fiber seen in Figure 27b at two magnifications

Figure 28 is a clearer instance of a fiber being exposed by the fracture. In this case, the fiber shows little to no amorphous regions. This microcrystalline cellulose structure is typical of a fiber that has been hydrolyzed to the point that the amorphous region is no longer visible, which benefits the mechanical properties of the fiber [85] [86]. With a diameter of about 10µm,

the base of the fiber shows no signs of voids, meaning that interfacial adhesion between matrix and fiber are appropriate to transfer stress onto the fiber. **Figure 28a** gives an image of the plastic deformation near the fiber where the small circular voids are signs of fiber pullout. In this case, the fibers, such as the one on the top left, exhibit more amorphous behavior, which reduces interfacial adhesion. Overall, it is safe to say that the functionalization of cotton produced a natural fiber reinforced composite with appropriate adhesion between components, but the hydrolyzation of cotton fibers was not uniform, as the extent of amorphous material present varied. The variation in fiber size and surface are one of the reasons for a ductile response rather than a more brittle one expected from adding reinforcements. Cotton fibers have a high specific strength, with a tensile strength in the range of 287-597 MPa despite their low density (1.5 g/cm) [49], which implies that the strength of the matrix should be increased through reinforcement. Nevertheless, the addition of fibers changes the fracture mode of the filament from a brittle one to a largely ductile one and more mechanical tests must be carried out to prove if this is making the material stronger or weaker when pulled in tension.

Finally, the indigo-cotton filaments are shown below. In this case, as in the DMA samples, there are various types of filaments that are included within this RPET-IC designation – a foamed specimen (**Fig.6.12 a** and **b**), a dark, translucent specimen (**Fig. 6.12 c**), and a dark specimen with agglomerations (**Fig. 6.12 d**). As can be seen in the images, the foamed specimen does not have the same geometry as the other filaments since there was excessive expansion during foaming. The fracture surface shows plastic deformation aligned with the tensile direction, which is in line with the ductile behavior exhibited in RPET-WC. In this case, exposed fibers of various thicknesses are also seen, and their presence despite the deformation also suggests that silanization helped the fibers adhere to the matrix properly, even with the indigo

present in the molecules. A closer look at the root of all deformation planes (**Fig. 6.12 b**) depicts a series of voids as the initiation sites of deformation with crazing evident in the light white sections.

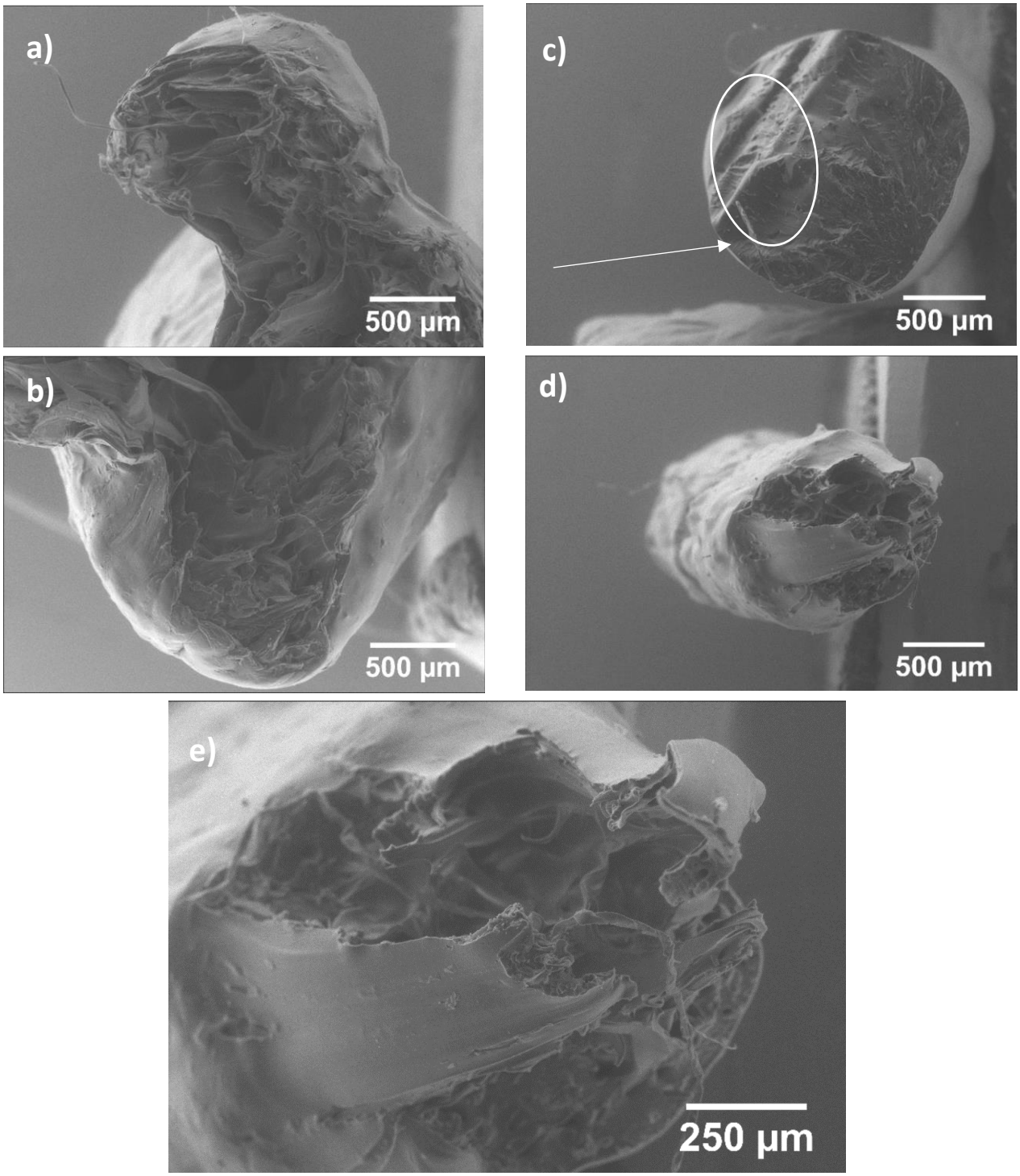

Figure 29: Low magnification RPET-IC fracture surfaces – a) and b) foam filament c) dark filament d) agglomerated filament and e) high magnification image of d)

On the other hand, the dark translucent filament in **Figure 29c** resembles the surface of pure RPET. The crack initiation site at the lower right section of the filament shows that crack propagation started in a brittle mode as hackle sections radiate out of this section. Towards the center of the filament, however, multiple pits are seen where fibers disrupted crack propagation. The distribution of these pits is evidence that fibers were evenly distributed in this section of filament.

One section in which fibers were not evenly dispersed and agglomeration was evident is **Figure 29d**, where even the length of the filament loses its uniformity where agglomerations affect the surface roughness. Towards the tip of the fracture surface, plastic deformation is evident as the outer skin of the filament was pulled towards the center where failure occurred. Between the sections of skin left behind, copious plastic deformation in the form of crazing occurred. Large voids within the filament similar to those of **Figure 26 a** show that the fracture mode of this filament was also a ductile one induced by large strain fields (**Figure 29e**), furthering the idea that the inclusion of cotton fibers is has a toughening effect on RPET.

Chapter 7: Conclusions

Overconsumption has led to a corresponding accumulation of solid waste. As virgin resources are increasingly exploited to keep up with consumption habits, waste continues to accumulate at alarming rates even though a large portion of said waste can be reused. This study presents a way to reuse two of the largest solid waste constituents found in landfills, cotton from textile waste and PET from plastic bottles through additive manufacturing technologies. Due to the compatibility of these two components (often exhibited in the use of textiles), they were selected as feedstock to produce a natural fiber reinforced polymer composite (NFRPC). Surface modifying techniques like acid hydrolysis and silane functionalization were carried out to make the cotton fibers more compatible with a recycled PET (RPET) matrix. Thermal extrusion processes mixed the composite, which was drawn into a 1.75mm monofilament to be printed through fused deposition modeling. Three filaments were extruded – an RPET baseline, a white cotton-RPET composite, and an indigo cotton-RPET composite with fibers obtained from post-consumer jeans.

Characterization of all three filaments through attenuated total reflectance (ATR) analysis showed that functionalization chemically changed the cotton fibers for the benefit of adhesion to the RPET matrix. Mixing in the extruder also altered the RPET matrix, as some peaks that were present in PET no longer appear in either filament. Furthermore, melt flow index (MFI) rheological studies hinted at a plasticizing effect of the fibers on the matrix as both composites had a higher MFI than the matrix. This drop in viscous behavior hints at either a decreased molecular weight or an improvement in molecular movement within the matrix due to fiber inclusions.

Fracture surfaces of all three filaments were examined under a scanning electron microscope (SEM) in variable pressure mode, which revealed a brittle fracture mode for RPET and a ductile one for both composites. Izod impact specimens were printed and tested for RPET and RPET-WC only because a failed extrusion attempt rendered the prepared RPET-IC filament unusable with the printer at hand. Test results confirm that the cotton fibers were toughening the matrix and increasing impact resistance. SEM images of impact fracture surfaces reveal an that fiber-matrix adhesion was enough to resist brittle fracture modes, especially since the evidence of pullout was minimal. Exposed fibers showed no sign of poor adhesion either.

Dynamic mechanical analysis (DMA) identified material response to stress at a range of temperatures for both RPET and RPET-WC. While the onset of rubbery response defined by a drop in storage modulus was lower for the RPET-WC composite, dampening (max tan δ) was increased. This is in line with the toughening effects seen through impact specimens.

The surge of additive manufacturing technologies over the last decade serves as an opportunity to create new material systems that may benefit society either through novel material systems never seen before or by providing a way to produce composite materials out of innovative system combinations. The latter is explored in this study with the hope of tackling two large contributors to solid waste – cotton from textiles and plastic bottles. As a proof of concept, this study shows that a NFRPC made with these constituents has attractive effects on mechanical properties of PET, namely the dampening characteristics and impact strength, but there is still much work that can be done to make the system more marketable at a large scale, which is why further research in innovative recycling methods is imperative.

7.1 Future Works

While this study proves that NFRPCs made with recycled cotton and plastic is possible, its complete characterization in terms of mechanical and thermal properties is still incomplete. Tensile strength tests are only one set of tests that will be used to further analyze this system in future studies. In addition, there is a lot of work to be done to improve pre-extrusion processing steps. For example, an automated cutting mill to extract fibers from denim cloth would increase amount of cotton that can be processed for a smaller workload. A simple way to implement this on a large scale is to use a drier and cycle multiple denim or 100% cotton articles until a decent amount of cotton fibers (lint) is collected for processing.

Mechanical properties would largely benefit from a more uniform hydrolyzing process so that all fibers have the same adhesive and mechanical properties throughout the system, so a case study here is also imperative. To prevent the extrusion issues that were seen in this iteration of the material's design, larger loads of the *pseudo-raw* materials will be processed to extrude with a twin-screw extruder, which will largely play a role in homogenizing the distribution of fibers throughout the matrix. Filament diameter consistencies will also benefit from this as the material can be better used in commercial printing.

Although they were implemented in this NFRPC to reinforce and benefit mechanical properties of the RPET, the cotton fibers also have other benefits that need further investigation. For example, as a polyester, PET is susceptible to hydrolytic chain scission in the presence of moisture. This hygroscopic response could potentially be dampened by treatments to the cotton fibers, or at the very least, the response to thermal conditions of the system need further exploration.

A complete characterization of NFRPCs made from recycled plastic and cotton also opens the door to comparing this system to other similar filaments in the market. For example, PET-G is a more attractive version of PET that is largely used in 3D printing because the glycolyzed version of PET has better flow properties and a suppressed crystallization [87]. The increase in MFI of the composites in this study suggest a similar effect on the RPET matrix, which is why crystallinity tests are another test to be conducted on the system.

Beyond simply being a competitive material in the world of material science, it is important to also verify that the production of this NFRPC is attractive in terms of energy used and life cycle analysis. There would not be much benefit to producing new products with this material if they shortly return to landfills to continue contaminating the Earth, so an analysis of how these materials interact with the environment, such biodegradability, are to also be conducted before claiming that they are truly a solution to the problem posed in the early chapters of this study. There is still much work to be done on the subject, but this study shows that it is possible to create an NFRPC with two recycled materials with the hope that a trend begins to look at waste as pseudo raw materials rather than a lost cause that is only left to decompose on its own.

7.1.1 Applications for Cotton-PET NFRPC

In order for the NFRP's production to have any impact on the accumulation of waste on landfills, its usage must become significant enough to disrupt the current trends. In other words, its applications must be as broad as possible, given that the goal is essentially to reuse as much waste as possible. While the applications of the NFRP are yet to be explored, suggestions based on literature of similar materials are plentiful. For example, Zander et al. proved that recycling PET bottles in the battlefield with AM technology provides a level of self-reliance that is important when material supplies are limited [76]. Given the abundance of both PET bottles and textile waste,

using a cotton-PET NFRPC such as the one presented here will give replacement parts produced in the battlefield a better toughness. Furthermore, the extrusion method used here to create a monofilament is not the only way to produce the composite. Injection molding is another way of production that will be explored in future works to see any differences in material properties. Another way to take advantage of the toughening properties of this NFRPC is to include it as a reinforcer for concrete composites. Teall et al. have done something similar to this by exploring the use of PET tendons as a "crack closure system within concrete … elements" [78]. Although the crack closure system is dependent on the shape memory properties of PET, which may have been altered with the addition of cotton, the NFRPC can certainly reinforce the concrete and act as a toughening agent. In conclusion, the applications to this material are plentiful, yet undefined with the intention of promoting its use across as many engineering fields as possible. After all, what matters with the development of this NFRPC is that it combats the accumulation of waste. A task that will only be fulfilled at a rate similar to the rate of accumulation.

References

[1] L. Blumberg and R. Gottlieb, War on Waste: Can America Win Its Battle with Garbage? - Louis Blumberg, Robert Gottlieb - Google Books, Island Press, 1989.

[2] J. Guiltinan, "Creative Destruction and Destructive Creations: Environmental Ethics and Planned Obsolescence," *Journal of Business Ethics,* vol. 89, no. 1, pp. 19-28, May 2009.

[3] V. Packard, The Waste Makers, G. a. C. L. Longmans, Ed., London: Lowe & Brydone Ltd, 1961.

[4] T. K. Aladeojebi, "Planned Obsolescence," *International Journal of Scientific & Engineering Research,* vol. 4, no. 6, 2013.

[5] R. Mason, "Ethics and the Supply of Status Goods," *Journal of Business Ethics,* vol. 4, no. 6, pp. 457-464, 1985.

[6] O. US EPA, "National Overview: Facts and Figures on Materials, Wastes and Recycling," 2015.

[7] O. US EPA, "Plastics: Material-Specific Data," 2015.

[8] J. R. Jambeck, R. Geyer, C. Wilcox, T. R. Siegler, M. Perryman, A. Andrady, R. Narayan and K. L. Law, "Plastic Waste Inputs from Land into the Ocean," *Science,* vol. 347, no. 6223, pp. 768-771, 2015.

[9] R. C. Thomspson, "Plastic Debris in the Marine Environment: Consequences and Solutions," *Marine Nature Conservation in Europe,* pp. 107-116, 2006.

[10] E. Fries, J. H. Dekiff, J. Willmeyer, M.-T. Nuelle, M. Ebert and D. Remy, "Identification of polymer types and additives in marine microplastic particles using pyrolysis-GC/MS and scanning electron microscopy †," *Environmental Science Processes & Impacts,* vol. 15, pp. 1949-1956, 8 August 2013.

[11] L. V. Cauwenberghe, "Microplastics in bivalves cultured for human consumption," *Environmental Pollution,* vol. 193, pp. 65-70, 2014.

[12] M. Liboiron, "Redefining pollution and action: The matter of plastics," *Journal of Material Culture,* vol. 21, no. 1, pp. 87-110, 2016.

[13] T. Nace, "We're Now At A Million Plastic Bottles Per Minute - 91% Of Which Are Not Recycled," 26 July 2017. [Online]. Available: https://www.forbes.com/sites/trevornace/2017/07/26/million-plastic-bottles-minute-91-not-recycled/#1a839450292c.

[14] T. Domina and K. Koch, "The Textile Waste Lifecycle," *Clothing and Textiles Research Journal,* vol. 15, no. 2, 1997.

[15] L. Claudio, "Environmental Impact of the Clothing Industry," *Environmental Health Perspectives,* vol. 115, no. 9, A 449- A454 September 2007.

[16] T. Lewis, "Apparel Disposal and Reuse," in *Sustainable Apparel: Production, Processing, and Recycling*, 1st ed., R. Blackburn, Ed., Woodhead Publishing Series in Textiles, 2015, pp. 233-250.

[17] C. Binotto and A. Payne, "The Poetics of Waste: Contemporary Fashion Practice in the Context of Wastefulness," *Fashion Practice,* vol. 9, no. 1, pp. 5-29, 2016.

[18] WRAP, "Valuing our Clothes," 2012.

[19] L. Norris, "Trade and Transformations of Secondhand Clothing: Introduction," *Textile: The Journal of Cloth and Culture,* vol. 10, no. 2, pp. 128-143, 2012.

[20] E. Stanes and C. Gibson, "Materials that linger: An embodied geography of polyester clothes," *Geoforum,* vol. 85, pp. 27-36, 10 2017.

[21] B. R. Babu, A. K. Parande, S. Raghu, T. Prem Kumar and T. P. Kumar, "TEXTILE TECHNOLOGY Cotton Textile Processing: Waste Generation and Effluent Treatment," *The Journal of Cotton Science,* vol. 11, pp. 141-153, 2007.

[22] I. E. Napper and R. C. Thompson, "Release of synthetic microplastic plastic fibres from domestic washing machines: Effects of fabric type and washing conditions," *MPB,* vol. 112, pp. 39-45, 2016.

[23] J. Szostak-Kotowa, "Biodeterioration of Textiles," *International Biodeterioration & Biodegradation,* vol. 53, pp. 165-170, 2004.

[24] R. J. Young and P. A. Lovell, "Concepts and Nomenclature," in *Introduction to Polymers*, Boca Raton, FL, Taylor & Francis Group, LLC, 2011, pp. 9-10.

[25] D. Whisnat, "Polymer Chemistry: Polymer Crystallinity," 2017. [Online]. Available: https://eng.libretexts.org/Bookshelves/Materials_Science/Supplemental_Modules_(Materials_Science)/Polymer_Chemistry/Polymer_Chemistry%3A_Morphology/Polymer_Chemistry%3A_Polymer_Crystallinity.

[26] "Glass Transition," [Online]. Available: https://pslc.ws/macrog/tg.htm.

[27] P. Debye, "Intrinsic Viscosity, Diffusion, and Sedimentation Rate of Polymers in Solution," *Polymer Solutions The Journal of Chemical Physics,* vol. 14, p. 2516, 1946.

[28] J. Zhang, A. Panwar, D. Bello, J. A. Isaacs, T. Jozokos and J. Mead, "The effects of recycling on the structure and properties of carbon nanotube-filled polycarbonate," *Polymer Engineering and Science,* vol. 58, no. 8, pp. 1278-1284, 04 August 2017.

[29] P. R. S. Dey, "An Overview of the Recent Trends in Manufacturing of Green Composites – Considerations and Challenges," *Materials Today: Proceedings,* vol. 5, no. 9, pp. 19783-19789, 2018.

[30] I. S. Duarte, A. A. Tavares, S. Lima, D. L. A. C. S. Andrade, L. H. Carvalho, E. L. Canedo, S. Edina and M. L. Silva, "Chain extension of virgin and recycled poly(ethylene terephthalate): Effect of processing conditions and reprocessing," *Polymer Degradation and Stability,* vol. 124, pp. 26-34, February 2016.

[31] P. Hayes, "Additives," in *Process Principles in Minerals and Materials Production*, Brisbane, Queensland, Australia, Hayes Publishing co, 2003, p. 440.

[32] J. E. McIntyre, "The Historical Development of Polyesters," in *Modern Polyesters: Chemistry and Technology of Polyesters and Copolyesters*, John Wiley & Sons, 2003, pp. 3-24.

[33] T. Rieckmann and S. Volker, "Poly(Ethylene Terephthalate) Polymerization – Mechanism, Catalysis, Kinetics, Mass Transfer and Reactor Design," in *Modern Polyesters: Chemistry and Technology of Polyesters and Copolyesters*, John Wiley & Sons, 2003, p. 59.

[34] T. Rieckmann and S. Volker, "Poly(Ethylene Terephthalate) Polymerization – Mechanism, Catalysis, Kinetics, Mass Transfer and Reactor Design," in *Modern*

Polyesters: Chemistry and Technology of Polyesters and Copolyesters, John Wiley & Sons, Ltd, 2003, p. 36.

[35] J. Rabek, "Oxidative Degradation of Polymers," in *Comprehensive Chemical Kinetics*, 1975, pp. 425-538.

[36] E. de Morais Teixeira, A. C. Corrêa, A. Manzoli, F. de Lima Leite, C. R. de Oliveira and L. H. C. Mattoso, "Cellulose nanofibers from white and naturally colored cotton fibers," *Cellulose,* vol. 17, no. 3, pp. 595-606, 12 June 2010.

[37] M. A. Said, A. Samir, F. Alloin and A. Dufresne, "Review of Recent Research into Cellulosic Whiskers, Their Properties and Their Application in Nanocomposite Field," *Biomacromolecules,* vol. 6, no. 2, pp. 612-626, 2005.

[38] X. Min Dong, J.-f. Ë Ois Revol and D. G. Gray Ã, "Effect of microcrystallite preparation conditions on the formation of colloid crystals of cellulose," *Cellulose,* vol. 5, pp. 19-32, 1998.

[39] E. S. Medeiros, L. H. C Mattoso, R. Bernardes-Filho, D. F. Wood and W. J. Orts, "Self-assembled films of cellulose nanofibrils and poly(o-ethoxyaniline)," *Colloid and Polymer Science,* vol. 286, no. 11, pp. 1265-1272, 2008.

[40] D. J. Gardner, G. S. Oporto, R. Mills and M. A. S. A. Samir, "Adhesion and Surface Issues in Cellulose and Nanocellulose," *Journal of Adhesion Science and Technology,* vol. 22, no. 5-6, pp. 545-567, 2008.

[41] M. Irimia-Vladu, E. D. Glowacki, P. A. Troshin, G. Schwabegger, L. Leonat, D. K. Susarova, O. Krystal, M. Ullah, Y. Kanbur, M. A. Bodea, V. F. Razumov, H. Sitter, S. Bauer and N. S. Sariciftci, "Indigo - A Natural Pigment for High Performance Ambipolar Organic Field Effect Transistors and Circuits," *Advanced Materials,* vol. 24, pp. 375-380, 2012.

[42] T. H. Courtney, "Composite Materials," in *Mechanical Behavior of Materials*, 2nd ed., New Delhi, McGraw Hill, 2000, pp. 244-289.

[43] T. H. Courtney, "Basic Principles of Reinforcement," in *Mechanical Behavior of Materials*, New Delhi, McGraw Hill, 2000, pp. 247-250.

[44] F. Hussain, M. Hojjati and R. E. Gorga, "Polymer-matrix Nanocomposites, Processing, Manufacturing, and Application: An Overview INTRODUCTION AND BACKGROUND," *Journal of COMPOSITE MATERIALS,* pp. 27-32, 2006.

[45] C. E. Bakis, Bank, L. C, F. Asce, Brown, V. L, M. Asce, Cosenza, E, Davalos, J. F, A. M. Asce, Lesko, J. J, Machida, A, Rizkalla, S. H and T. C. Triantafillou, "Fiber-Reinforced Polymer Composites for Construction-State-of-the-Art Review," *Journal of Composites for Construction,* vol. 6, no. 2, 2002.

[46] A. Brink, "Thermoplastic Polyester Composites," in *Modern Polyesters: Chemistry and Technology of Polyesters and Copolyesters*, John Wiley & Sons, 2003, pp. 542-549.

[47] M. Fazeli, J. P. Florez and R. A. Simão, "Improvement in adhesion of cellulose fibers to the thermoplastic starch matrix by plasma treatment modification," *Composites Part B: Engineering,* vol. 163, pp. 207-216, April 2019.

[48] S. N. Monteiro, F. P. D. Lopes, A. S. Ferreira and D. C. O. Nascimento, "Natural-fiber polymer-matrix composites: Cheaper, tougher, and environmentally friendly," *The*

Journal of The Minerals, Metals & Materials Society (TMS), vol. 61, no. 1, pp. 17-22, 2009.

[49] X. Li, A. E. A. G. T. Lope and S. Panigrahi, "Chemical Treatments of Natural Fiber for Use in Natural Fiber-Reinforced Composites: A Review," *Journal of Polymers and the Environment,* vol. 15, no. 1, pp. 25-33, 2007.

[50] A. Keller, "Compounding and mechanical properties of biodegradable hemp fibre composites," *Composite Science and Technology,* vol. 63, no. 9, pp. 1307-1316, 2003.

[51] R. Sepe, F. Bollino, L. Boccarusso and F. Caputo, "Influence of chemical treatments on mechanical properties of hemp fiber reinforced composites," *Composites Part B: Engineering,* vol. 133, pp. 210-217, 2018.

[52] "Overview Polymer-Matrix Composites," 21 April 2019. [Online]. Available: www.tms.org/jom.html.

[53] J. Thomason, "The interface region in glass fibre-reinforced epoxy resin composites: 1. Sample preparation, void content and interfacial strength," *Composites,* pp. 467-475, 1995.

[54] O. Onuaguluchi and N. Banthia, "Plant-based natural fibre reinforced cement composites: A review," *Cement and Concrete Composites,* vol. 68, no. 4, pp. 96-108, 2016.

[55] A. Atiqah, M. Jawaid, M. R. Ishak and S. M. Sapuan, "Effect of Alkali and Silane Treatments on Mechanical and Interfacial Bonding Strength of Sugar Palm Fibers with Thermoplastic Polyurethane," *Journal of Natural Fibers,* vol. 15, no. 2, pp. 251-261, 2018.

[56] B. A.N. and N. K.J., "Characterization of alkali treated and untreated new cellulosic fiber from Saharan aloe vera cactus leaves," *Carbohydrate Polymers,* vol. 174, pp. 200-208, 2017.

[57] H. Ku, H. Wang, N. Pattarachaiyakoop and M. Trada, "A review on the tensile properties of natural fiber reinforced polymer composites," *Composites Part B: Engineering,* vol. 42, no. 4, pp. 856-873, 2011.

[58] A. Valadez-Gonzalez, J. M. Cervantes-Uc, R. Olayo and P. J. Herrera-Franco, "Effect of fiber surface treatment on the fiber-matrix bond strength of natural fiber reinforced composites," *Composites Part B: Engineering,* vol. 30, no. 3, pp. 309-320, 1999.

[59] T. H. Courtney, "Reinforcement with Discontinuous Fibers," in *Mechanical Behavior of Materials*, 2nd ed., New Delhi, McGraw Hill, 2000, pp. 257-263.

[60] A. Gebhardt and J.-S. Hötter, "Characteristics of the Additive Manufacturing Process," in *Additive Manufacturing: 3D Printing for Prototyping and Manufacturing*, 2016, pp. 21-91.

[61] T. F. Horn and O. L. Harrysson, "Overview of current additive manufacturing technologies and selected applications," *Science Progress,* vol. 95, no. 3, pp. 255-282, 2012.

[62] D. A. Roberson, A. R. Torrado Perez, C. M. Shemelya, A. Rivera, E. MacDonald and R. B. Wicker, "Comparison of stress concentrator fabrication for 3D printed polymeric izod impact test specimens," *Additive Manufacturing,* pp. 1-11, 2015.

[63] C. I. Chung, "Physical Description of Single-Screw Extrusion," in *Extrusion of Polymers Theory & Practice*, Cincinnati, Hanser Publications, 2000.

[64] D. Rosato, "The Complete Extrusion Process," in *Extruding Plastics: A practical processing handbook - D.V. Rosato - Google Books*, Springer Science & Business Media, 1998.

[65] R. Chokshi and H. Zia, "Hot-Melt Extrusion Technique: A Review," *Iranian Journal of Pharmaceutical Research,* vol. 3, pp. 3-16, 2004.

[66] J. R. Wagner Jr., E. M. Mount III and H. F. Giles Jr., "Extrusion Process," in *Extrusion: The Definitive Processing Guide and Handbook*, 2014, p. 3–11.

[67] J. Wagner Jr., M. E. Mount III and H. F. Giles Jr., "Twin Screw Extrusion Process," in *Extrusion: The Definitive Processing Guide and Handbook*, 2014, pp. 111-120.

[68] J. R. Wagner Jr., E. M. Mount III and H. F. Giles Jr., "Plastic Behavior in the Extruder," in *Extrusion: The Definitive Processing Guide and Handbook*, 2014, p. 47–70.

[69] J. Wagner Jr., E. Mount III and H. Giles Jr., "Polymer Rheology," in *Extrusion: The Definitive Processing Guide and Handbook*, 2014, p. 233–240.

[70] O. S. Es-Said, J. Foyos, R. Noorani, M. Mendelson, R. Marloth and B. A. Pregger, "Effect of Layer Orientation on Mechanical Properties of Rapid Prototyped Samples," *Materials and Manufacturing Processes,* vol. 15, no. 1, pp. 107-122, 2000.

[71] A. R. Torrado, C. M. Shemelya, J. D. English, Y. Lin, R. B. Wicker and D. A. Roberson, "Characterizing the effect of additives to ABS on the mechanical property anisotropy of specimens fabricated by material extrusion 3D printing," *Additive Manufacturing,* vol. 6, pp. 16-29, April 2015.

[72] A. Hrymak, V. Bravo, Y. Khalfalla and K. Benyounis, "Polymer Melt Mixing in Twin Screw Extruders," *Elsevier: Reference Module in Materials Science and Engineering,* 2016.

[73] A. Torrado Perez, D. Roberson and W. R, "Fracture Surface Analysis of 3D-Printed Tensile Specimens of Novel ABS-Based Materials," *Journal of Failure Analysis and Prevention,* vol. 14, no. 3, pp. 343-353, June 2014.

[74] A. Kearns, N. Farahbakhsh, R. Venditti and J. Jur, "Cotton Fibers in 3D Printing," in *Solid Freeform Fabrication*, 2016.

[75] R. Araújo, F. L., C. Rezende, M. Marques, M. Errico, R. Avolio, M. Avella, G. Gentile and P. Russo, "Poly(lactic acid)/Cellulose Composites Obtained from Modified Cotton Fibers by Successive Acid Hydrolysis," *Journal of Polymers and the Environment,* vol. 26, no. 8, pp. 3149-3158, 12 August 2018.

[76] N. E. Zander, M. Gillan and R. H. Lambeth, "Recycled polyethylene terephthalate as a new FFF feedstock material," *Additive Manufacturing,* vol. 21, pp. 174-182, 2018.

[77] Y.-H. Kim, J. Jang, K.-G. Song, E.-S. Lee and S.-W. Ko, "Durable flame-retardant treatment of polyethylene terephthalate (PET) and PET/cotton blend using dichlorotribromophenyl phosphate as new flame retardant for polyester," *Journal of Applied Polymer Science,* vol. 81, no. 4, pp. 793-799, 25 July 2001.

[78] O. Teall, M. Pilegis, J. Sweeney, T. Gough, G. Thompson, A. Jefferson, R. Lark and D. Gardner, "Development of high shrinkage polyethylene terephthalate (PET) shape memory polymer tendons for concrete crack closure," *Smart Materials and Structures,* vol. 26, no. 4, 2017.

[79] P. Salminen, "Using recycled polyethylene terephthalate (PET) in the production of bottle trays," 2013.

[80] ASTM International, "ASTM D1238-04 Standard Test Method for Melt Flow Rates of Thermoplastics by Extrusion Plastometer 1".

[81] B. Demirel, A. Yaraş and H. Elçiçek, "Crystallization Behavior of PET Materials," *BAÜ Fen Bil. Enst. Dergisi Cilt,* vol. 13, no. 1, pp. 26-35, 2011.

[82] ASTM International, "ASTM D256 - 10 Standard Test Methods for Determining the Izod Pendulum Impact Resistance of Plastics," 2010.

[83] K. Menard and B. Bilyeu, "Dynamic Mechanical Analysis of Polymers and Rubbers," *Encyclopedia of Analytical Chemistry: Applications, Theory and Instrumentation,* 29 September 2008.

[84] I. A. Carrete, D. Bermudez, C. Aguirre and e. al, "Failure Analysis of Additively Manufactured Polyester Test Specimens Exposed to Various Liquid Media," *Journal of Failure Analysis and Prevention,* vol. 19, no. 2, pp. 418-430, 2019.

[85] K. Das, D. Ray, N. Bandyopadhyay, T. Ghosh, A. Mohanty and M. Misra, "A study of the mechanical, thermal and morphological properties of microcrystalline cellulose particles prepared from cotton slivers using different acid concentrations," *Cellulose,* vol. 16, no. 5, pp. 783-793, 2009.

[86] M. Haafiz, A. Hassan, Z. Zakaria, I. Inuwa, M. Islam and M. Jawaid, "Properties of polylactic acid composites reinforced with oil palm biomass microcrystalline cellulose," *Carbohydrate Polymers,* vol. 98, no. 1, pp. 139-145, 2013.

[87] R. B. Dupaix and M. C. Boyce, "Finite strain behavior of poly(ethylene terephthalate) (PET) and poly(ethylene terephthalate)-glycol (PETG)," *Polymer,* vol. 46, no. 13, pp. 4827-4838, 2005.

[88] J. R. WagnerJr, E. M. MountIII and H. F. GilesJr., "Twin Screw Extruder Equipment," in *Extrusion: The Definitive Processing Guide and Handbook*, 2014, pp. 125-148.

[89] W. J. Orts, J. Shey, S. H. Imam, G. M. Glenn, M. E. Guttman and J.-F. Revol, "Application of Cellulose Microfibrils in Polymer Nanocomposites," *Journal of Polymers and the Environment,* vol. 13, no. 4, pp. 301-306, 2005.

[90] C. Binotto and A. Payne, "The Poetics of Waste: Contemporary Fashion Practice in the Context of Wastefulness," *Fashion Practice,* vol. 9, no. 1, pp. 5-29, 2016.

Curriculum Vita

Israel Alejandro Carrete was born in Ciudad Juarez, Chihuahua and raised in El Paso, Texas. After graduating from Socorro High School in 2013, he attended Brown University, where he completed his Bachelor of Science in Materials Engineering in 2017. During his tenure at Brown, Israel dabbled in advocacy for underrepresented students in STEM and dedicated much of his time to mentoring underclassmen to ensure retention in engineering was improved. While most of his summer activities at Brown were dedicated to research with Dr. Guduru, he also worked as the Head of Sustainability for CamisasTex – a tech startup dedicated to reducing textile waste in the Boston area.

After the completion of his bachelor's degree, Israel returned to his home town and volunteered at the local Fabrication Laboratory (FabLab) before pursuing his Master's degree at the University of Texas at El Paso (UTEP). Once in UTEP, Israel became a member of the Dr. Roberson's Polymers Extrusion Lab, where he published the articles cited below (two more are to be published as of the time of this writing).

Following this venture, Israel looks towards expanding his knowledge in materials to the discipline of industrial design. He will pursue a Master of Science degree in Integrated Product Design at the Delft University of Technology (TU Delft). The change in disciplines comes with the hope to merge the two disciplines into one that revitalizes the design process in a more responsible and environmentally friendly manner.

Contact Information: iacarrete@gmail.com